

1 **Abstract**

2 Microalgae are known as good producers of high-added value bioproducts useful in many
3 applications such as pharmaceuticals, nutrition or biofuel production. In contrast to
4 phototrophy, heterotrophy emerges as a promising strategy for algal biomass production due
5 to high cell densities, controlled conditions and reduced space requirement. Hemicellulose is
6 the second most abundant material in land plants. Its hydrolysis liberates xylose, glucose,
7 acetate. Our study focuses on three microalgal species, *Galdieria sulphuraria*, *Euglena gracilis*,
8 and *Auxenochlorella protothecoides*, cultivated under heterotrophy with the above-
9 mentioned carbon sources, supplemented alone or in combination. Growth parameters and
10 biomass analysis revealed distinctive characteristics. *G. sulphuraria*, despite a modest fatty
11 acid content (5-15% w/w), displayed potential for hemicellulose valorization, demonstrating
12 high biomass yield using xylose as a sole carbon source (approx. 0.5 gDW g_{xylose}⁻¹) and high
13 saturated fatty acid (SFA) content (45-63%). In our cultivation conditions, *E. gracilis* only
14 assimilated acetate with low fatty acid content (approx. 6% w/w), but high SFA content (60-
15 77%) and high paramylon content (47% w/w), convertible to wax-esters under anaerobiosis.
16 *A. protothecoides* exhibited biomass yields of 0.42-0.54 gDW g_{substrate}⁻¹ depending on the
17 carbon substrate supplied but maintained constant fatty acid content (16-18% w/w) in the
18 presence of all substrates except xylose. Surprisingly, despite an inability to grow with xylose
19 alone, sugar depletion analysis indicated decreasing xylose concentration when other carbon
20 sources were present in the cultivation medium for this alga. This comparative study discusses
21 the strengths and weaknesses of each strain, providing insights into their potential when
22 grown on hemicellulose carbon sources.

23

1 Introduction

2 Microalgae are widely studied across various fields such as human nutrition, pharmacology,
3 bioremediation, and biofuel production [1–3]. Certain microalgal species exhibit the ability to
4 grow heterotrophically, utilizing carbon molecules from their environment in the absence of
5 light. Heterotrophic growth offers several advantages over phototrophic growth, including
6 better monitoring over culture conditions, reduced risk of contamination as a consequence
7 of indoor and closed cultivation systems, and typically higher growth rates [4–7]. Additionally,
8 heterotrophic microalgae often show increased accumulation of reserve polysaccharides [8–
9 13] and higher lipid content and/or productivity [7,14–17]. Furthermore, the absence of light
10 generally reduces the pigment [18–21] and protein contents [13,22–24]. These nitrogenous
11 compounds can affect the costs of the biomass conversion process into biofuel, and the oil
12 quality by the production of nitrogen oxides (NO_x) during combustion [25–28].

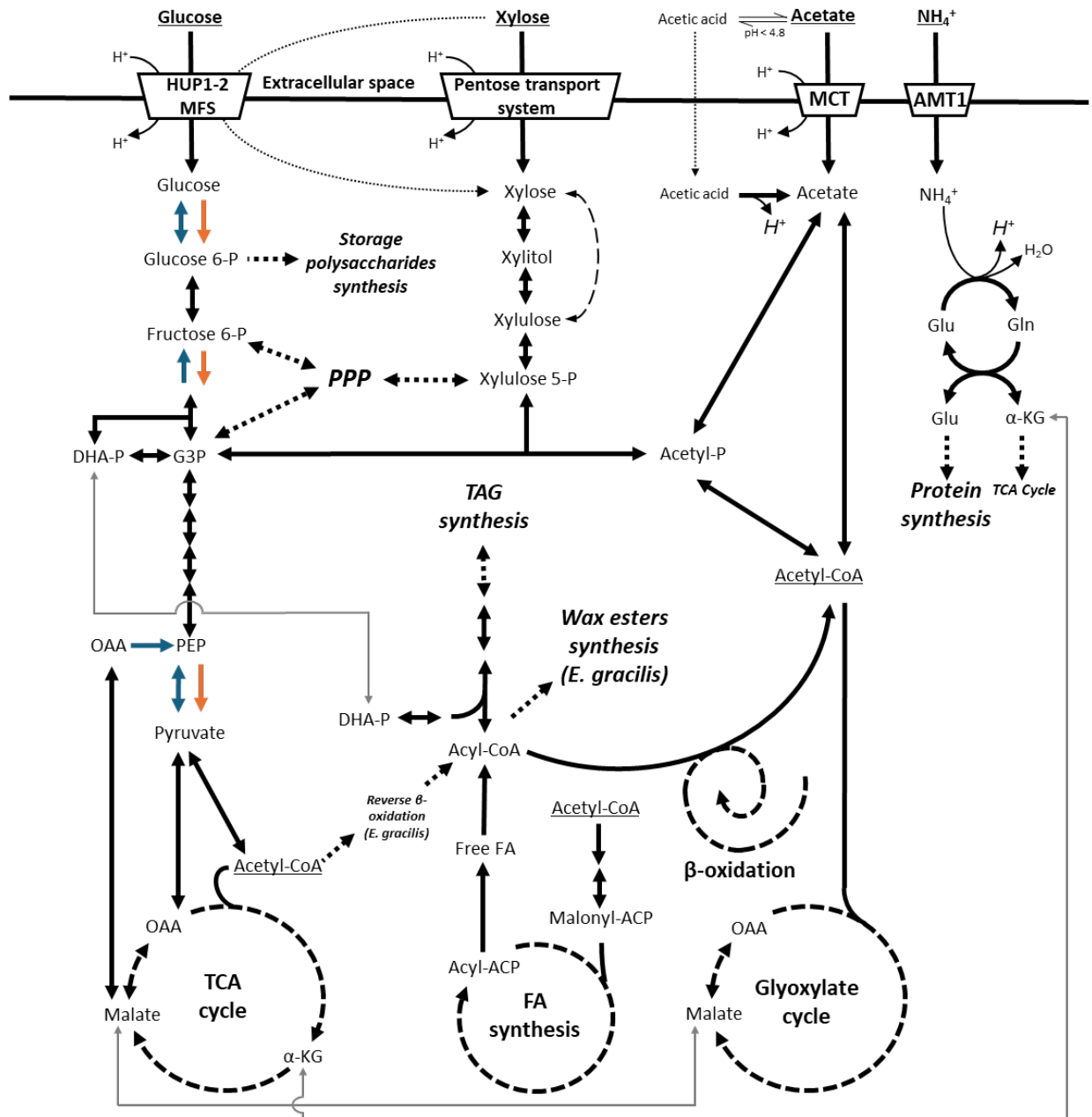
13 However, the utilization of carbon sources such as glucose for microalgal growth raises ethical
14 concerns when derived from biomass cultivated on arable lands. Nonetheless, these carbon
15 compounds can also originate from renewable feedstock like agricultural wastes, straw, or
16 from forestry operations [29–31]. The organic matter originating from such industries
17 primarily comprises cellulose, along with a substantial amount of hemicellulose, considered
18 the second most prevalent family of compounds in plant biomass [32]. Once completely
19 hydrolyzed using thermochemical methods, hemicellulose releases various carbon
20 compounds, predominantly xylose (5-25 g L⁻¹), glucose (1-25 g L⁻¹), and acetate (2-8 g L⁻¹)
21 [33,34]. Although glucose and acetate are known to be suitable for heterotrophic growth of
22 many microalgae, xylose, despite being the most abundant sugars on Earth after glucose
23 (accounting for 18-30% of lignocellulose hydrolysate sugars) is rarely metabolized [35]. Once

1 translocated into the cell via Major Facilitator Family (MSF) transporters or hexose/H⁺
2 symporter systems [20,36], glucose can be phosphorylated to enter glycolysis or pathways for
3 reserve or structural polysaccharide biosynthesis [37–39]. Acetate, on the other hand, can
4 either passively diffuse through the plasma membrane in its acetic acid form or utilize proton-
5 linked MonoCarboxylate Transporters (MCTs) before being converted into acetyl-CoA [38–
6 40]. This central molecule of energy metabolism can then participate in fatty acid synthesis
7 or enter the glyoxylate and the tricarboxylic acid (TCA) cycle or undergo gluconeogenesis to
8 form hexoses [40]. Xylose, meanwhile, uses specific pentose transporters in some species,
9 while in others it utilizes transporters normally intended for hexoses [41]. Subsequently, it is
10 redirected to various metabolic pathways such as the pentose phosphate pathway (PPP)
11 and/or glycolysis after its conversion to xylitol, then xylulose, and finally xylulose 5-P [42] (**Fig.**
12 **1**). Only a few microalgae species have shown effective growth on sole xylose [41,43,44], and
13 even fewer can use the three aforementioned carbon sources as feedstock. This is likely
14 because most photosynthetic organisms lack specific transporters for their assimilation [45–
15 48]. Among heterotrophic microalgal species, we decided to focus on three strains originating
16 from different phyla and able to convert the carbon sources found in hemicellulose into algal
17 biomass intended for various applications. We selected *Galdieria sulphuraria*, a red microalga
18 (Rhodophyta) known for its ability to assimilate numerous different carbon sources under
19 heterotrophic conditions while being capable of reaching high biomass concentrations
20 [49,50]. Additionally, *G. sulphuraria* can produce high levels of saturated fatty acids (SFAs),
21 known to be favorable for biofuel production [51,52]. Also, *G. sulphuraria* accumulates
22 significant amounts of a particular type of glycogen, stored in the cytosol, and called floridean
23 starch, studied in health, nutrition, and in the fermentation-based synthesis of certain types
24 of biofuels [10,53,54].

1 We also conducted our research on the Euglenozoa *Euglena gracilis*, for its capacity to
2 assimilate acetate and glucose [13,55]. Furthermore, lacking a cell wall, its cellular content is
3 easily accessible for industrial purposes. *E. gracilis* accumulates paramylon within the cytosol
4 as storage polysaccharide, that is insoluble in water and imparting unique properties in the
5 medical fields such as immunity [9,12,56]. Moreover, in addition to produce high levels of
6 SFAs, *E. gracilis* paramylon is converted into wax esters under anoxic conditions, which are
7 highly favorable to produce medium-chain biofuels such as biodiesel or biokerosene
8 [14,57,58].

9 Lastly, we investigated *Auxenochlorella protothecoides*, a green alga of the genus *Chlorella*. It
10 is known to reach high biomass densities in heterotrophy in the presence of various carbon
11 sources [4–7], but also for its flexibility of growth conditions, and its relevance in 3rd
12 generation biomass production for biofuel synthesis [5,7]. Indeed, the *Chlorella* genus is one
13 of the most studied for biofuel production due to the ability of some strains to exhibit high
14 lipid content (up to 50% of the total DW in some cases for *A. protothecoides* grown in
15 heterotrophy) [4,7,29,59], while producing few reserve of polysaccharides and pigments
16 [4,7,29,59].

17 In this article, we investigated the growth of the three microalgae—*G. sulphuraria*, *E. gracilis*,
18 and *A. protothecoides*—in the presence of the main carbon sources found in hemicellulose
19 hydrolysate, namely glucose, acetate, and xylose, as well as in an equimolar mixture of the
20 three. Additionally, we measured their biomass content and composition to evaluate their
21 potential applications, particularly in the field of biofuels.



1

2 **Figure 1:** Schematic representation of the uptake and metabolism of glucose, xylose, acetate, and ammonium (NH_4^+) in
 3 microalgae, based on [14,20,36–42,60]. Black arrows indicate specific enzymatic reactions leading to the subsequent
 4 products (enzyme names and co-substrates are generally not specified). Black arrows crossing trapezoids represent
 5 transporters. Small gray arrows connect single compounds that can be transferred from one pathway to another. Circular
 6 dashed arrows represent metabolic cycles (with intermediate products and enzymatic reactions not shown), and straight
 7 dashed arrows indicate entry points into specific metabolic pathways written in bold and italics, which are not necessarily
 8 detailed. Orange and blue arrows mark specific reactions of glycolysis and gluconeogenesis, respectively. The dashed arrows
 9 connecting xylose to xylulose omitting the xylitol intermediate represent the putative presence of a xylose isomerase, as
 10 already characterized in bacteria [61]. Compound abbreviations are specified as follows: α -KG, α -ketoglutarate; ACP, acyl
 11 carrier protein; AMT1, ammonium transporter 1; CoA, coenzyme A; DHA-P, dihydroxyacetone phosphate; FA, fatty acid; G3P,
 12 glyceraldehyde 3-P; Gln, glutamine; Glu, glutamate; HUP1-2, hexose uptake protein; MCT, monocarboxylate transporters;
 13 MFS, major facilitator superfamily; PEP, phosphoenolpyruvate; PPP, pentose phosphate pathway; TAG, triacylglycerol; TCA,
 14 tricarboxylic acid. The locations where metabolic reactions occur have intentionally not been specified, as they may differ
 15 depending on the species studied.

16

1 **Materials and methods**

2 **Microalgal strains, culture media, and precultures**

3 *G. sulphuraria* strain 074 was obtained from the algal Collection at the University Federico II (ACUF)
4 ([http://www.acuf.net/index.php?option=com_content&view=article&id=520:galdieria-sulphuraria-](http://www.acuf.net/index.php?option=com_content&view=article&id=520:galdieria-sulphuraria-galdieri-merola24&catid=2&Itemid=127&lang=en&Itemid=113)
5 [galdieri-merola24&catid=2&Itemid=127&lang=en&Itemid=113](http://www.acuf.net/index.php?option=com_content&view=article&id=520:galdieria-sulphuraria-galdieri-merola24&catid=2&Itemid=127&lang=en&Itemid=113)). The strain corresponds to the 074W
6 isolate described in [49] and previously described in [20]. The strain was maintained axenically at 25°C
7 under constant illumination ($40 \mu\text{mol}_{\text{photon}} \text{m}^{-2} \text{s}^{-1}$) on a sterile agar plate containing 2xGS modified
8 Allen medium [62] (**Table 1**). One liter of 2xGS Allen medium contains: 1.5 g $(\text{NH}_4)_2\text{SO}_4$, 300 mg
9 $\text{MgSO}_4 \cdot 7\text{H}_2\text{O}$, 300 mg $\text{KH}_2\text{PO}_4 \cdot 2\text{H}_2\text{O}$, 20 mg $\text{CaCl}_2 \cdot 2\text{H}_2\text{O}$, 19.9 mg NaCl, 13.2 mg Fe-Na-EDTA, 5.72 mg
10 H_3BO_3 , 3.64 mg $\text{MnCl}_2 \cdot 4\text{H}_2\text{O}$, 0.44 μg $\text{ZnSO}_4 \cdot 7\text{H}_2\text{O}$, 2.1 mg $(\text{NH}_4)_6\text{Mo}_7\text{O}_{24} \cdot 4\text{H}_2\text{O}$, 0.1 mg $\text{CuSO}_4 \cdot 5\text{H}_2\text{O}$,
11 0.05 mg $\text{NaVO}_3 \cdot 4\text{H}_2\text{O}$ and 44 μg $\text{CoCl}_2 \cdot 6\text{H}_2\text{O}$. pH was adjusted to 2.0 with 96% H_2SO_4 prior to
12 sterilization by autoclaving the medium for 20 min at 121°C. For solid 2xGS Allen medium, 500 mL with
13 2% agar were mixed with a 2-times concentrated medium after autoclaving and being cooled down to
14 around 60°C to achieve 1% agar plates.

15 *E. gracilis* SAG 1224-5/25 (**strain Z**) and *A. protothecoides* SAG 211-7a strains were obtained from the
16 Culture Collection of Algae at Göttingen University, Germany (SAG). Both strains were maintained
17 axenically at 25°C under constant illumination ($40 \mu\text{mol}_{\text{photon}} \text{m}^{-2} \text{s}^{-1}$) on agar plates containing Tris-
18 Minimal-Phosphate (TMP) medium [63] (**Table 1**). One liter of TMP medium contains: 2.42g Tris buffer,
19 400 mg NH_4Cl , 50 mg $\text{CaCl}_2 \cdot 2\text{H}_2\text{O}$, 100 mg $\text{MgSO}_4 \cdot 7\text{H}_2\text{O}$, 93.5 mg K_2HPO_4 , 63.0 mg KH_2PO_4 , 50 mg Na_2 -
20 $\text{EDTA} \cdot 2\text{H}_2\text{O}$, 22 mg $\text{ZnSO}_4 \cdot 7\text{H}_2\text{O}$, 11.4 mg H_3BO_3 , 5.1 mg $\text{MnCl}_2 \cdot 4\text{H}_2\text{O}$, 4.9 mg $\text{FeSO}_4 \cdot 7\text{H}_2\text{O}$, 1.6 mg
21 $\text{CoCl}_2 \cdot 6\text{H}_2\text{O}$, 1.6 mg $\text{CuSO}_4 \cdot 5\text{H}_2\text{O}$ and 1.1 mg $(\text{NH}_4)_6\text{Mo}_7\text{O}_{24} \cdot 4\text{H}_2\text{O}$. pH was adjusted to 7.0 with 37% HCl
22 prior to sterilization by autoclaving the medium for 20 min at 121°C. For solid TMP medium, 15 g of
23 agar were added to the solution before sterilization to achieve 1.5% agar plates. After sterilization,
24 the medium was supplemented with thiamine (vitamin B_1) at a concentration of 10 μM for *A.*

1 *protothecoides* and with a mix of biotin (vitamin B₈, 100 nM), cobalamin (vitamin B₁₂, 100 nM), and
 2 thiamine (10 µM) for *E. gracilis* cultivation, respectively.

3 **Table 1.** Comparison of the molecules and elements concentrations between the 2xGS Allen and TMP media. Values are
 4 expressed in molar units (M) and do not include pH adjustment. NF: the compound is not found in the medium.

Compound	Medium	
	TMP	2xGS Allen
TRIS	$2 \cdot 10^{-2}$	NF
Mg ²⁺	$4.06 \cdot 10^{-4}$	$1.22 \cdot 10^{-2}$
SO ₄ ²⁻	$5.06 \cdot 10^{-4}$	$1.26 \cdot 10^{-2}$
Ca ²⁺	$3.40 \cdot 10^{-4}$	$1.36 \cdot 10^{-4}$
Cl ⁻	$8.19 \cdot 10^{-3}$	$6.50 \cdot 10^{-4}$
K ⁺	$1.54 \cdot 10^{-3}$	$2.20 \cdot 10^{-3}$
PO ₄ ³⁻	$1.00 \cdot 10^{-3}$	$2.20 \cdot 10^{-3}$
NH ₄ ⁺	$7.49 \cdot 10^{-3}$	$2.27 \cdot 10^{-2}$
EDTA	$1.71 \cdot 10^{-4}$	$3.60 \cdot 10^{-5}$
BO ₃ ³⁻	$1.84 \cdot 10^{-4}$	$9.25 \cdot 10^{-5}$
Fe ²⁺	$1.76 \cdot 10^{-5}$	$3.60 \cdot 10^{-5}$
Cu ²⁺	$6.29 \cdot 10^{-6}$	$6.40 \cdot 10^{-7}$
Zn ²⁺	$7.65 \cdot 10^{-5}$	$1.54 \cdot 10^{-5}$
Mn ²⁺	$2.56 \cdot 10^{-5}$	$1.84 \cdot 10^{-5}$
Co ²⁺	$6.77 \cdot 10^{-6}$	$3.36 \cdot 10^{-7}$
Mo ₇ O ₂₄ ⁶⁻	$8.90 \cdot 10^{-7}$	$1.70 \cdot 10^{-6}$
Na ⁺	NF	$3.76 \cdot 10^{-4}$
VO ₃ ⁻	NF	$4.12 \cdot 10^{-7}$

5
 6 For the three strains, cells grown on agar plates were used to inoculate liquid phototrophic precultures
 7 that were maintained in 250 mL flasks with 70 mL of medium under constant shaking and LED-
 8 illumination ($100 \mu\text{mol}_{\text{photon}} \text{m}^{-2} \text{s}^{-1}$) at 25°C (*E. gracilis* and *A. protothecoides*) or 42°C (*G. sulphuraria*)
 9 in an incubator (GroBanks®, CLF Plant Climatics, Germany or Memmert GmbH, Germany,
 10 respectively). Before the experiments, cells were adapted to heterotrophy as described in the
 11 following section **Growth conditions and harvesting**. Heterotrophic precultures were maintained in
 12 the dark in an incubator at the same temperature as for phototrophic precultures under constant
 13 shaking for 10 days. Adaptation step was performed a second time using the first heterotrophic
 14 preculture as inoculum, when the conditions permitted growth.

15

1 **Growth conditions and harvesting**

2 All strains were grown in the dark in 250 mL flasks containing 70 mL of medium in an incubator under
3 constant shaking with specific temperature and culture medium, as described for the precultures. The
4 four tested conditions for each strain were different regarding the nature of the carbon source
5 supplemented to the medium: 25 mM of glucose, 30 mM of xylose, 75 mM of sodium acetate or a mix
6 of the three carbon sources (8.33 mM of glucose, 10 mM of xylose, 25 mM of sodium acetate). The
7 carbon sources were added to the cultivation media to reach a final concentration of 150 mM of
8 carbon atoms (mMC). The flasks were inoculated with two-times heterotrophically adapted cells pre-
9 cultivated on the same carbon source as the tested condition, at a starting OD₈₀₀ of 0.2. All strains and
10 culture conditions were performed in three independent biological replicates.

11 Once or twice a day, culture medium samples were harvested for algal growth measurements. 2-25
12 mL of culture were harvested and centrifuged (16,000 x g; 3min) to recover the algal cells for pigments,
13 proteins, storage polysaccharides (glycogen, paramylon or starch), and lipids quantification. Samples
14 were frozen at -20°C if the analysis was not performed directly. At the end of the culture, the
15 remaining volume served for biomass estimation.

16 All cultures were monitored until growth arrest, generally due to the assimilable carbon source
17 depletion, since other elements such as ammonium and phosphate were supplied in excess and were
18 never spotted as depleted at the end of growth (**Fig. S1**).

19 Additional analyses on *E. gracilis* cells adapted to heterotrophic conditions were conducted using
20 Koren-Hutner (KH) [64] and TMP media. The cells were grown at 25°C in the dark with constant
21 agitation in 100 mL flasks with 25 mL of medium. Each medium was supplemented with 50 mMC of
22 either acetate or glucose with an initial pH of 3.5 or 7.5 and cultures were maintained for 7 days. The
23 experiments were performed with two independent biological replicates, starting with an inoculum
24 of 125.000 dark-adapted cells per mL.

1 Algal growth measurements, biomass determination and growth parameter calculation

2 Algal growth was determined at least once a day measuring the OD₈₀₀ spectrophotometrically (Perkin-
3 Elmer lambda™ 265 UV/VIS, USA) in cuvettes of an optical path of 1 cm. Dilutions are performed to
4 maintain an absorbance value between 0.1 and 0.3. The dry biomass (DW) concentration was
5 estimated upon OD measurements using an OD/DW ratio calculated at the end of the culture for each
6 strain and carbon source. When no growth was observed in a specific condition, an OD/DW ratio from
7 another condition was used for biomass estimation. Biomass was measured by harvesting 15-30 mL
8 of algal culture that were centrifuged (4,000 x g; 3min), washed twice in distilled water, and
9 transferred in pre-weighted aluminum cup. After 24 h in a 70°C oven, the aluminum cups were then
10 weighted to gravimetrically estimate the DW.

11 Specific growth rate (μ) expressed in day⁻¹ as the slope of the linear regression of the natural log dry
12 weight number as a function of time in exponential phase as follows:

$$13 \quad \mu = \frac{\ln OD_{800_2} - \ln OD_{800_1}}{t_2 - t_1}$$

14 Biomass productivity, expressed in DW L⁻¹ d⁻¹, was calculated as follows:

$$15 \quad DW \text{ productivity} = \frac{DW_2 - DW_1}{t_2 - t_1}$$

16 Biomass yield ($Y_{x/s}$) on substrate, expressed in gDW g_{substrate}⁻¹, was calculated as follows:

$$17 \quad Y_{x/s} = \frac{X_{max} - X_0}{S_0 - S_1}$$

18 Where X_{max} represents the maximal DW concentration and X_0 the DW concentration (g L⁻¹) at the start
19 of the culture. S_0/S_1 represent the carbon source concentration (g L⁻¹) at the start and at the end of
20 the culture, respectively.

21 Xylose biomass yield in the mix condition for *A. protothecoides* ($Y_{x/xylose}$), expressed in gDW g_{xylose}⁻¹, was
22 estimated as follows:

$$Y_{x/xylose} = \frac{Xmax_{mix} - (Xth_{glucose} + Xth_{acetate})}{[xylose]_0 - [xylose]_1}$$

The theoretical glucose ($Xth_{glucose}$) and acetate ($Xth_{acetate}$) contributions as carbon source to the maximal DW concentration (gDW L⁻¹) were extrapolated as follows:

$$Xth_{glucose} = ([glucose]_0 - [glucose]_1) \times Y_{x/glucose}$$

5

$$Xth_{acetate} = ([acetate]_0 - [acetate]_1) \times Y_{x/acetate}$$

Where $[xylose]_0/[xylose]_1$, $[glucose]_0/[glucose]_1$, and $[acetate]_0/[acetate]_1$ are the carbon source concentrations (g L⁻¹) at the start and at the end of the culture, respectively. $Xmax_{mix}$ (gDW L⁻¹) represents the maximal DW concentration in the mix condition. $Y_{x/glucose}$ and $Y_{x/acetate}$ (gDW g⁻¹) are the biomass yields of *A. protothecoides* calculated based on the glucose and acetate conditions, respectively.

Cell count of additional analyses on *E. gracilis* grown on KH or TMP medium was performed using a Thoma counting chamber.

14 pH measurement and nutrient quantification

For pH, carbon source, ammonium, and phosphate quantification, 2 mL of culture medium were harvested and centrifuged (16,000 x g; 3min). Supernatant was stored at -20°C before quantification.

pH. pH was measured in 1 mL of culture supernatant using a pH-meter probe (HANNAH® instruments Edge® Dedicated pH Meter, USA).

Carbon sources. Glucose, xylose and acetate concentrations in the culture supernatant were quantified by High Performance Liquid Chromatography (HPLC, Shimadzu, Japan) as described in [20]. Concentrations were determined based on the peak area of the chromatogram, compared to standard curves of known glucose, acetate, or xylose concentrations. Injection volume was 40 µL for all samples.

1 **Ammonium.** Ammonium concentration in the culture medium was determined using the enzymatic
2 method provided by the Megazyme® Ammonia Assay Kit (Rapid) (Neogen® corporation, USA) in 96-
3 well plate. Concentrations were calculated based on a standard curve of known NH₄Cl concentrations
4 ranged between 0 and 1 µg of NH₄⁺ per well.

5 **Phosphate.** The determination of the phosphate concentration in the culture medium was based on
6 a colorimetric method from [65] performed in a 96-well plate and already described in a previous
7 paper [20]. Concentrations were calculated based on a standard curve of known KH₂PO₄
8 concentrations ranged between 0 and 0.75 mM of PO₄³⁻ per well.

9 **Pigment quantification.** Hydrophobic pigments were separated by HPLC (Shimadzu, Japan) using a
10 reverse-phase C18 column (Nova-Pak silica column, 3.9 x 150 mm, 4 µm particle size, Waters, USA)
11 and detected with a photodiode array detector SPD-M20A (PDA, Shimadzu, Japan) as previously
12 described [20]. The identity of each pigment was determined based on the retention time and the
13 specific absorbance spectrum in the visible light. Quantification was done by comparison with pure
14 pigments at different concentrations (DHI Lab Products, Denmark). Injection volume was ranged
15 between 10-100 µL for all samples. Pigment content was normalized on the dry biomass
16 concentration.

17 **Hydrophilic pigments.** Phycocyanin concentration in *G. sulphuraria* cells was estimated
18 spectrophotometrically (Perkin-Elmer lambda™ 265 UV/VIS, USA) as described previously in [20]. The
19 blue supernatant was used to calculate the phycocyanin concentration spectrophotometrically with
20 the formulas reported in [66]. Phycocyanin content was normalized on the dry biomass concentration.

21 **Protein quantification.** Protein concentration of frozen pelleted cells (2-4 mL of culture) was
22 quantified using a RC DC™ Protein Assays kit (BioRad, USA) based on a modified Lowry assay [67], that
23 is detergent compatible as described previously [20]. Concentrations were calculated based on a
24 standard curve of known bovine serum albumin (BSA) concentrations ranged between 0 and 3 mg mL⁻¹

1 ¹ of the solubilization solution mentioned above. Protein content was normalized on the dry biomass
2 concentration.

3 **Glycogen, paramylon and starch quantification.** Paramylon content in *E. gracilis* was quantified using
4 a colorimetric method based on the phenol-sulfuric acid assay [68]. 5-10 mL of culture pellet were
5 washed twice in TMP without carbon source and resuspended in 1 mL of Tris-acetate buffer (25 mM,
6 pH7.5). 0.5 mm Ø glass beads were added to the tubes and cells were disrupted with a TissueLyzer II
7 (Qiagen, Netherlands) for 5 min at 30Hz. Cell debris were washed twice in Tris-acetate buffer (25 mM,
8 pH7.5) and pelleted (800 x g, 10 min) into a new 2 mL test tube. To separate the insoluble paramylon
9 from the cell debris, the pellet was resuspended in 1 mL of 80% Percoll[®] solution and transferred on
10 the top of 1 mL of 80% Percoll[®] solution in a 2 mL test tube. The samples were centrifuged at 10,000
11 x g for 10 min and the supernatant containing the debris was discarded. The paramylon-rich pellet
12 was washed twice with distilled water to eliminate the Percoll[®] and finally resuspended in 500 µL
13 distilled water. 40 µL of each sample were placed in a 96-well plate with dilutions from 1 to 1/128 to
14 fit in the standard curve range, before adding 20 µL of 5% phenol solution and 100 µL of H₂SO₄ 95-
15 98% to each well. After an incubation at 80°C for 45 min, the absorbance of the 96-well plate was read
16 spectrophotometrically at 490 nm (Synergy Mx, Biotek Instruments, Inc., USA). Paramylon
17 concentrations were calculated based on a standard curve of known glucose concentrations ranged
18 between 0 and 0.3 g L⁻¹. The final paramylon concentration was normalized on the dry biomass
19 concentration. Glycogen in *G. sulphuraria* or starch in *A. protothecoides* were determined with an
20 enzymatic method as previously described in [20], with some modifications. All enzymes were
21 provided by Megazyme[®] (Neogen[®] corporation, USA). 2-4 mL of culture were pelleted and washed
22 twice in the culture medium with no carbon source. Cells were disrupted with a TissueLyzer II (Qiagen,
23 Netherlands) for 2x10 min at 30Hz (5 min break on ice between the two lysing steps) in the presence
24 of 700 µL of Tris-acetate buffer (50 mM, pH 7.5) and 0.5 mm Ø glass beads. Samples were then
25 centrifuged (16,000 x g; 5 min) and the supernatant (containing soluble starch or glycogen) was

1 transferred into a new 1.5 mL tube. DMSO 20% were added to the insoluble starch-containing pellet.
2 Megazyme® thermostable α -amylase (10-times diluted in 100 mM acetate buffer, pH 5) was added to
3 all samples (insoluble in DMSO 20% and soluble) and the tubes were placed at 99°C for 10 min under
4 constant agitation. During this step, the insoluble starch could be solubilized. Samples were
5 centrifuged and the supernatant was transferred into a 96-well plate. Samples were then incubated
6 for 30 min at 58°C Megazyme® Amyloglucosidase from *Aspergillus niger* was used to break the α -1,4-
7 glycosidic bonds. In the presence of NADP and ATP, 100 μ L of a Megazyme® mix of hexokinase and
8 glucose-6-phosphate dehydrogenase generated one molecule of 6-phospho-gluconolactone and one
9 molecule of NADPH per molecule of glucose. NADPH formation was measured at 340 nm
10 spectrophotometrically (Synergy Mx, Biotek Instruments, Inc., USA). Soluble starch (or glycogen) and
11 insoluble starch concentrations were calculated based on a standard curve of known glucose
12 concentrations ranged between 0 and 1 g L⁻¹. The final starch or glycogen concentration was calculated
13 by summing the soluble and insoluble fractions. This total storage polysaccharide concentration was
14 normalized on the dry biomass concentration.

15 **Fatty Acid Methyl Esters (FAMES) quantification.** Fatty acids quantification and distribution were
16 determined as previously described in [20,69]. 2-4 mL of culture were pelleted and resuspended in
17 chloroform/methanol (2:1, v/v). The quantification of FAMES was based on the peak area, using an
18 external calibration curve realized with a FAMES mix, suitable for microalgae fatty acids determination
19 (Supelco37, Sigma-Aldrich, USA). Total fatty acid content was calculated by summing all the separated
20 FAMES concentrations. Fatty acid content was normalized on the dry biomass concentration.

21

1 **Results and discussion**

2 All the data for *G. sulphuraria* grown on glucose are from a previous study conducted by the present
3 research group and can be found in the following article : [20].

4 **Growth parameters analysis**

5 **(i) With glucose**

6 In this study, *E. gracilis* was cultivated under neutral pH conditions. This choice was made
7 because, at pH values below 5, certain organic acids including formate, propionate, butyrate,
8 and acetate (the latter being particularly relevant here as it is a component of hemicellulose
9 hydrolysate)- exist in their lethal non-dissociated forms [70,71]. This consideration is further
10 discussed in section (iv) which addresses the assimilation of glucose, xylose, and acetate.
11 Unfortunately, *E. gracilis* did not grow in the presence of glucose under the tested culture
12 conditions (**Fig. 2A**). This result is surprising since, even if growth rates are slightly lower
13 compared to the low pH conditions (pH 3.5-5) [71–74], growth in the presence of glucose at
14 pH close to 7 has been reported in various studies [71–74]. This prompted us to conduct
15 additional experiments on two media: TMP and KH [58] at pH levels of 3.5 and 7.5. The results
16 demonstrated that *E. gracilis* strain Z is unable to grow on glucose on TMP at either pH
17 (**Supplemental Table S2**). In contrast, the strain can grow on glucose in the KH medium, but
18 only at pH 3.5. As expected, neither KH nor TMP sustain growth on acetate at pH 3.5 due to
19 the toxicity of acetate at acidic pH levels (**Table S2** and discussion below). A key component
20 present in KH and a significant factor in *E. gracilis* (strain Z) growth on glucose, but absent in
21 TMP, is citrate [24,71]. Some studies have found that sodium citrate, even if not assimilated,
22 may play an important chelating role in glucose metabolism during neutral pH adaptation, as
23 no growth was observed in a mineral medium containing only glucose as carbon source [75].

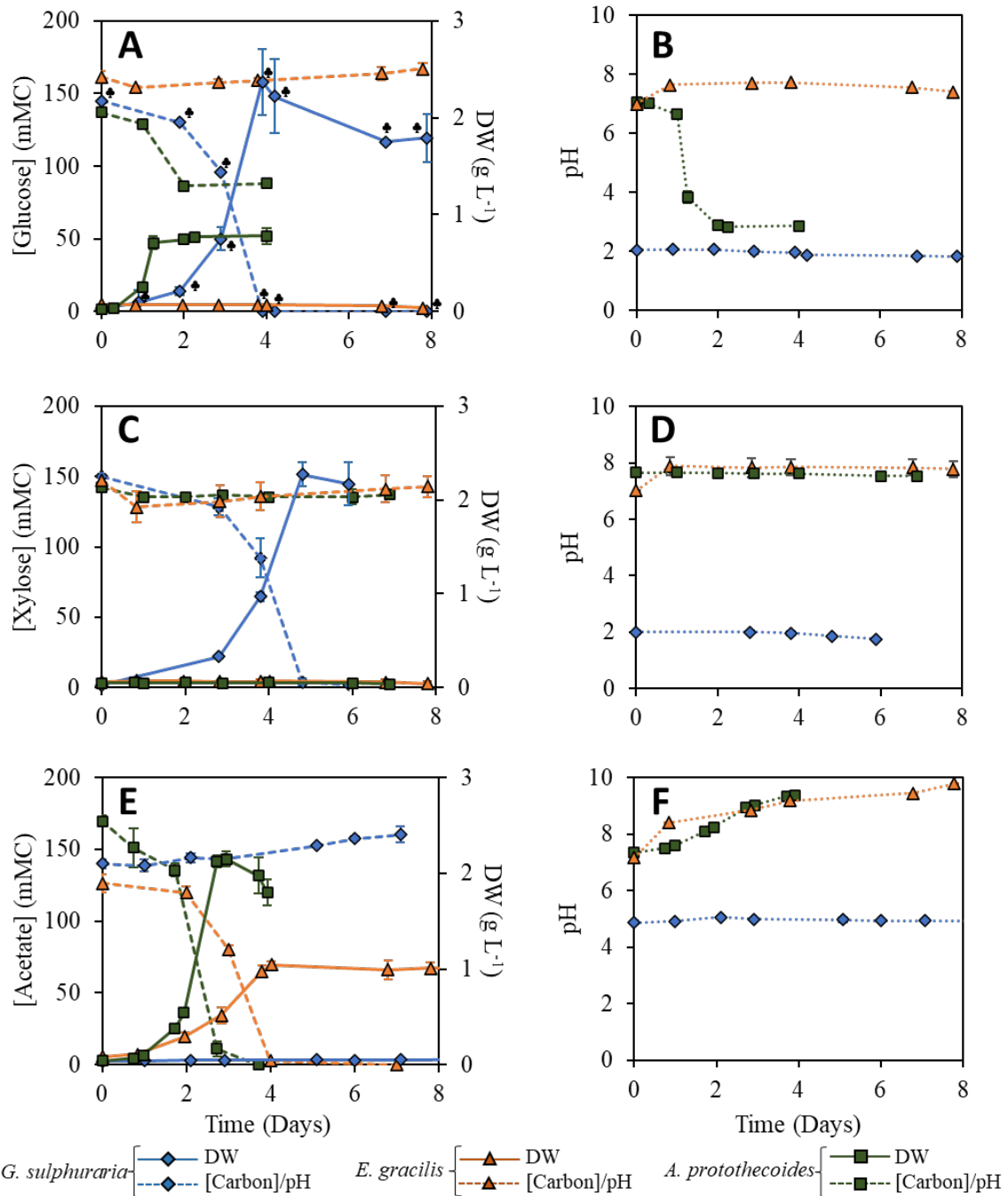
1 A similar observation was made when citrate (50 mg.L^{-1}) was replaced by EDTA (10 mg.L^{-1}),
2 suggesting that a chelating agent may be necessary for glucose assimilation at pH 7.0 [75].
3 The TMP-medium used in this study contains EDTA at a concentration of 50 mg.L^{-1} , which may
4 be slightly too high to effectively promote glucose assimilation as the same study found that
5 a concentration of 100 mg.L^{-1} of EDTA did not have a positive effect in the same context [75].
6 Chelators likely facilitate the entry of essential metallic ions in the cell and/or capture
7 inhibitory heavy metals. However, their exact role in carbon metabolism remains unclear, as
8 they are not required for acetate assimilation (see section (iii) on acetate). Further
9 experiments could be conducted using TMP medium supplemented with citrate to evaluate
10 the importance of this molecule in the context of glucose assimilation. Since the aim of the
11 paper is growth analysis on a mix of the three carbon sources mentioned previously, including
12 acetate, the choice of the TMP medium for both *E. gracilis* and *A. protothecoides* is relevant.

13 In contrast, as already shown in a previous study conducted in the laboratory [20] and
14 reported here for comparison, *G. sulphuraria* showed a specific growth rate (μ) of 1.10 ± 0.03
15 d^{-1} , a maximum biomass productivity yield of $1.62 \pm 0.22 \text{ gDW L}^{-1} \text{ d}^{-1}$, a maximal biomass
16 production of $2.37 \pm 0.34 \text{ g L}^{-1}$ and a biomass yield ($Y_{x/s}$) of $0.53 \pm 0.08 \text{ gDW g}_{\text{substrate}}^{-1}$ in the
17 presence of glucose (**Fig. 2A; Table 2**). After 4 days of culture, the stationary phase was
18 reached due to glucose depletion. These growth parameters are similar to those reported in
19 the literature [30]. Finally, *A. protothecoides* showed an exponential growth in the presence
20 of glucose only during the first day but with exceptionally high growth parameters compared
21 to the literature [29,76,77]: a specific growth rate of $3.29 \pm 0.01 \text{ d}^{-1}$, a maximum biomass
22 productivity yield of $1.77 \pm 0.22 \text{ gDW L}^{-1} \text{ d}^{-1}$ and a biomass yield of $0.54 \pm 0.04 \text{ gDW g}^{-1}$,
23 comparable to *G. sulphuraria* (**Table 2**). However, the growth stopped abruptly at day 2. By
24 the end of the culture only about 50 mM C have been consumed (**Fig. 2A**), resulting in low

1 biomass production ($0.78 \pm 0.08 \text{ g L}^{-1}$) compared to the other species of this study (**Table 2**).
2 Given that the the growth of most *Chlorella* species is typically compromised at pH levels
3 below 5 [77–80], we suggest that the growth arrest observed in *A. protothecoides* cells
4 cultivated with glucose is likely due to rapid medium acidification during glucose
5 consumption.

6 Effectively, glucose consumption lowers the pH in both *G. sulphuraria* and *A. protothecoides*
7 cultures, dropping from 2.05 ± 0.02 to 1.83 ± 0.03 and from 7.05 ± 0.03 to 2.87 ± 0.05 ,
8 respectively (**Fig. 2B**). Such pH imbalance was reported before in similar conditions [69,70]
9 and can result from various factors, one of which is the production of CO_2 in response to
10 respiratory metabolism, leading to a decrease in pH due to the molecule dissolution in water,
11 forming carbonic acid that dissociates into bicarbonate and protons [60]. Therefore, it can be
12 inferred that the accumulation of CO_2 , triggered by the rapid growth rate of the algae (**Table**
13 **2**) in the presence of glucose, played a significant role in the acidification of the culture
14 medium. Another significant process contributing to pH acidification could be the metabolism
15 of ammonium through the GS-GOGAT pathway (**Fig. 1**), wherein a proton is released into the
16 medium for every assimilated ammonium molecule [60]. To address the problem of medium
17 acidification that is lethal to most *Chlorella* species, another buffer like PIPES with a lower pKa
18 ($\text{pKa}=6.76$) than the Tris used in this study ($\text{pKa}=8.3$) could be used or an automatic pH
19 monitoring [78,82]. Additionally, many *Chlorella* species can assimilate nitrate, which, unlike
20 ammonia, tends to raise pH with non-lethal effects [60,77,81].

21



1

2 **Figure 2:** Growth curves, and evolution of carbon sources concentration and pH in the culture media of *G. sulphuraria* (light
3 blue diamonds), *E. gracilis* (orange triangles), and *A. protothecoides* (dark green squares) cells grown in heterotrophy in the
4 presence of glucose (A-B), xylose (C-D), or acetate (E-F). Graphs (A,C,E) show dry weight evolution (gDW L⁻¹ - solid lines,
5 secondary vertical axis) and carbon source concentration in the media (mM of carbon atoms - dashed lines, primary vertical
6 axis) over time (days). Graphs (B,D,F) show the pH evolution in cultures (pH units - dashed lines, primary horizontal axis) over
7 time (days). Each value on the graphs is presented as the mean of three independent biological replicates. Error bars
8 represent standard deviation of the mean (± SD). The clover symbol (♣) indicates values for *G. sulphuraria* grown on glucose
9 from a previous study conducted in our laboratory [20].

10

1 (ii) With xylose

2 In the presence of xylose assimilation as sole carbon source in heterotrophy no growth was
3 observed for both *E. gracilis* and *A. protothecoides*, as reported previously [76,83] (**Fig. 2C**).
4 In contrast, *G. sulphuraria* was able of growing in the presence of xylose as sole carbon source
5 (**Fig. 2C**). Exponential phase lasted 5 days, with a specific growth rate of $0.97 \pm 0.03 \text{ d}^{-1}$, a
6 biomass yield of $0.51 \pm 0.01 \text{ gDW g}^{-1}$, and a maximum biomass productivity of 1.31 ± 0.08
7 $\text{gDW L}^{-1} \text{ d}^{-1}$. These results are comparable to those mentioned in [30], except for the biomass
8 yield that is about 30% higher in this case, indicating that xylose can be used as an effective
9 carbon source by *G. sulphuraria* for biomass production (**Table 2**). With *G. sulphuraria* apart,
10 to the best of our knowledge, *C. sorokiniana* and some *Scenedesmaceae* such as *Scenedesmus*
11 *quadricauda* are exceptions that demonstrated xylose uptake when used as the sole carbon
12 source in heterotrophic condition [41,43,44]. Nevertheless, compared to the mentioned
13 xylose-metabolizing species, *G. sulphuraria* stands out as the most promising microalga for
14 converting xylose into biomass.

15 (iii) With acetate

16 *G. sulphuraria* did not grow in the presence of acetate. At the beginning of the culture, the
17 addition of 75 mM sodium acetate to the pH 2 medium leads to a pH increase to
18 approximately 5 due to the buffering action of the acetate/acetic acid buffer system, where
19 acetate ions react with hydronium ions, consuming them and thereby elevating the pH while
20 remaining within the buffering range ($\text{pKa}=4.8$) (**Fig. 2F**) [84]. Given that a pH superior to 5
21 impedes *G. sulphuraria* growth, we attempted to lower the pH to 2 using sulfuric acid after
22 the addition of sodium acetate. Nonetheless, adjusting the pH had no positive effect on
23 growth and acetate assimilation, indicating that *G. sulphuraria* is not able to use acetate as

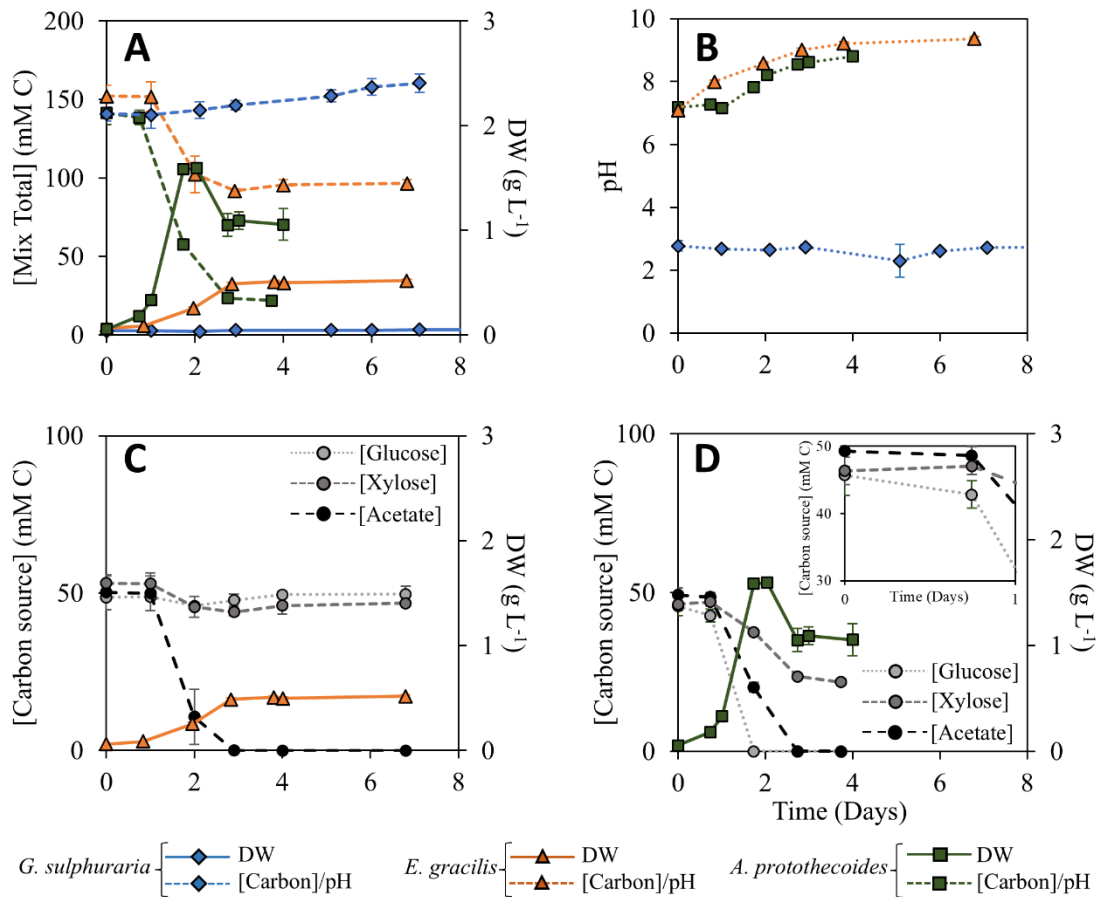
1 sole carbon source. *A. protothecoides* was capable of more efficient acetate assimilation and
2 metabolization than *E. gracilis* since specific growth rates of $1.74 \pm 0.09 \text{ d}^{-1}$ and $0.73 \pm 0.02 \text{ d}^{-1}$,
3 and biomass yield of 0.42 ± 0.02 and $0.26 \pm 0.02 \text{ gDW g}^{-1}$ were monitored, for a total of 2
4 and 3 days of exponential phase, respectively (**Fig. 2E; Table 2**). The specific growth rate for
5 *E. gracilis* was lower compared to other studies on the same strain. For instance, a specific
6 growth rate of 1.28 d^{-1} was obtained in [71], but with a significantly reduced biomass yield of
7 0.11 g.g^{-1} on an inorganic medium supplemented with 30 mM of acetate. Due to the toxicity
8 of acetate at pH levels below pKa (4.8), the researchers confirmed that biomass production
9 was optimal at nearly neutral pH, with little variation observed between pH 6 to 9 [71].
10 Acetate consumption resulted in a pH elevation for both *E. gracilis* and *A. protothecoides*
11 raising the pH of the culture from 7.16 ± 0.01 to 9.78 ± 0.02 and 7.33 ± 0.03 to 9.36 ± 0.03 ,
12 respectively (**Fig. 2F**). pH elevation during acetate consumption has been reported in other
13 studies as well [40,71,84]. Like for glucose which enters the cell using the hexose/H⁺ symport
14 system [36], acetate uptake into the cytoplasm is also accompanied by the uptake of a proton
15 via the monocarboxylate/proton symport (MCT) system [37,85]. Nevertheless, since acetate
16 and glucose have two and six carbon atoms, respectively, acetate transportation will tend to
17 remove 3-times more H⁺ to the cultivation medium for an equivalent amount of carbon atoms
18 assimilated. This might be the primary reason for such pH elevation during acetate
19 metabolization.

20 **(iv) In a mix of glucose, acetate and xylose**

21 The final condition investigated was an equimolar mixture of the three previously mentioned
22 carbon sources. Even if the condition does not exactly mimic the composition of hardwood
23 hemicellulose hydrolysate [34], it gives an insight of the ability of each strain to grow in the

1 presence of such substrate. *G. sulphuraria* did not grow under this condition, despite the
2 presence of glucose and xylose that could be assimilated when provided alone (**Fig. 3A**).
3 Acetate toxicity in acidic conditions has been demonstrated in various microorganisms such
4 as fungi, bacteria, archaea, and microalgae [40,70,71,86–90]. An acidic environment such as
5 the low pH (pH=2) used for optimal *G. sulphuraria* or *E. gracilis* growth, promotes the
6 formation of acetic acid. Contrary to their dissociated form, the non-dissociated form of some
7 organic acids, directly related to their lipophilic nature when protonated, diffuse passively
8 through the cell membrane contrary to free protons that are blocked by diverse mechanisms
9 in acidophilic organisms [91]. The consequence is an acidification of the cytosol, perturbing
10 the proton gradient used for ATP synthesis [40] and enzymatic reactions [91,92]. Other
11 studies on the heterotrophic growth of *G. sulphuraria* have also shown growth inhibition in
12 the presence of low amounts of organic acids such as acetate and butyrate [30,89].
13 Experiments on *G. sulphuraria* strain UTEX 2919 on a mixture of glucose and acetate revealed
14 similar results, demonstrating that glucose consumption and growth were inhibited in the
15 presence of acetic acid in concentrations superior to 0.6 g L⁻¹ (approx. 10 mM) [30]. However,
16 below that threshold, representing around 40% of the tested acetate concentration in this
17 study (25 mM), the *G. sulphuraria* was able to detoxify the medium and even metabolize
18 acetic acid, prior to start glucose consumption [30]. Organic acid consumption and
19 detoxification has already been shown in other acidophilic microorganisms such as archaea
20 species, but seems to be limited to low organic acids concentrations [90,91]. Another study,
21 focusing on the utilization of a wide range of carbon sources by *G. sulphuraria* 074G in the
22 presence of light, shows that not all organic acids are toxic, since malic and citric acids had
23 either a negative or positive effect on growth compared to phototrophic growth [88]. In
24 addition, among the variety of the tested carbon sources (hexoses, pentoses, polyols and

1 amino acids), none of them triggered growth inhibition. These results suggest that toxicity of
 2 the carbon source is truly mediated by the lipophilic nature of the non-dissociated form of
 3 some molecule such as organic acids at in low pH conditions [88].



5 **Figure 3:** Growth curves, and evolution of carbon sources concentration and pH in the culture media of *G. sulphuraria* (light
 6 blue diamonds), *E. gracilis* (orange triangles), and *A. protothecoides* (dark green squares) cells grown in heterotrophy in the
 7 presence of a mix of glucose, xylose and acetate (A-D). Graphs (A) shows dry weight evolution (gDW L^{-1} - solid lines, secondary
 8 vertical axis) and carbon source concentrations in the media (mM of total carbon atoms - dashed lines, primary vertical axis)
 9 over time (days). Graphs (B) show the pH evolution in cultures (pH units - dashed lines, primary vertical axis) over time (days).
 10 Graphs (C) and (D) show the glucose (dashed line, light gray circles) xylose (dashed line, dark gray circles), and acetate (dashed
 11 line, black circles) consumption (mM of carbon atoms – primary vertical axis) over time (days) in cultures of *E. gracilis* or *A.*
 12 *protothecoides*, respectively. In graph (D), the inset shows the carbon source evolution from day 0 to day 1. Each value on
 13 the graphs is presented as the mean of three independent biological replicates. Error bars represent standard deviation of
 14 the mean (\pm SD).

15 *E. gracilis*, as expected from the other conditions, did not consume glucose and efficiently
 16 assimilated acetate with a comparable biomass yield as with acetate alone ($0.28 \pm 0.04 \text{ gDW}$
 17 g^{-1}) (Fig. 2A; Table 2). However, a slight decrease in xylose concentration from 53.15 ± 2.34
 18 mM to 44.00 ± 1.17 mM was observed between day 1 and day 3 (Fig. 3C). While xylitol

1 uptake has been shown to support the growth of *E. gracilis* in mixotrophic conditions [93], to
2 the best of our knowledge, xylose diminution in heterotrophic cultivation conditions has not
3 been previously reported for Euglenoids. Given that some xylose-containing polysaccharides
4 are present in the cell composition of *E. gracilis* [94,95], it is plausible that this alga can recycle
5 xylose-containing compounds [95]. Nonetheless, since no xylose was consumed when present
6 as the sole carbon source, it suggests that the main challenge lies in xylose transport through
7 the cell membrane. This assumption raises questions about how xylose uptake was facilitated
8 in this condition. Further experiments using ^{13}C -labeled xylose should be conducted to
9 confirm xylose uptake and metabolization, or to understand the xylose concentration
10 decrease within the cultivation medium.

11 *A. protothecoides* was the only candidate able to metabolize the three carbon sources when
12 provided together and efficient growth was observed, lasting 2 days before growth arrest (**Fig.**
13 **3A,D**). As expected from the cultures conducted with the carbon sources alone, glucose and
14 acetate were consumed, leading to comparable biomass yield to acetate conditions ($0.43 \pm$
15 0.02 gDW g^{-1} for the mix and $0.42 \pm 0.02 \text{ gDW g}^{-1}$ with acetate) (**Table 2**) and a specific growth
16 rate slightly higher than with acetate alone, but far from that observed with glucose ($1.94 \pm$
17 0.04 d^{-1} for the mix, $3.29 \pm 0.01 \text{ d}^{-1}$ with glucose and $1.74 \pm 0.09 \text{ d}^{-1}$ with acetate). As can be
18 seen in **Fig. 3D**, glucose was preferentially consumed over acetate since glucose is depleted
19 between day 1 and day 2, when acetate is still present. Because of the lack of sampling
20 between these two points, it is not possible to determine if acetate uptake starts before or
21 after complete glucose depletion. These observations remind the carbon catabolite
22 repression (CCR) found in many microorganisms such as bacteria [83] and yeasts [98–100]
23 which usually leads to a preference for consuming glucose or acetate over 'secondary' carbon
24 sources. Nevertheless, there is no clear evidence that such a mechanism can occur in *A.*

1 *protothecoides*. Experiments in the presence of acetate and a non-metabolized glucose
 2 analogue like 2-deoxy-d-glucose should be performed to either demonstrate a CCR
 3 mechanism or to show that the assimilation rate is specific the carbon source catabolism.

4 **Table 2:** Growth parameters of *G. sulphuraria*, *E. gracilis*, or *A. protothecoides* in the presence of different substrates. Data
 5 are presented as means of three independent biological replicates \pm SD. NG: no growth was observed for that strain and
 6 condition. The clover symbol (♣) indicates values for *G. sulphuraria* grown on glucose from a previous study conducted in
 7 our laboratory [20].
 8

Carbon substrate	Strain	Specific growth rate μ (d ⁻¹)	Max DW (g L ⁻¹)	Max DW productivity (gDW L ⁻¹ d ⁻¹)	Biomass yield
					$Y_{(x/y)}$ (gDW g _{substrate} ⁻¹)
Glucose	<i>G. sulphuraria</i>	1.10 \pm 0.03 ♣	2.37 \pm 0.34 ♣	1.62 \pm 0.22 ♣	0.53 \pm 0.08 ♣
	<i>A. protothecoides</i>	3.29 \pm 0.01	0.78 \pm 0.08	1.77 \pm 0.22	0.54 \pm 0.04
	<i>E. gracilis</i>	NG	NG	NG	NG
Xylose	<i>G. sulphuraria</i>	0.97 \pm 0.03	2.27 \pm 0.13	1.31 \pm 0.08	0.51 \pm 0.01
	<i>A. protothecoides</i>	NG	NG	NG	NG
	<i>E. gracilis</i>	NG	NG	NG	NG
Acetate	<i>G. sulphuraria</i>	NG	NG	NG	NG
	<i>A. protothecoides</i>	1.74 \pm 0.09	2.15 \pm 0.08	2.00 \pm 0.03	0.42 \pm 0.02
	<i>E. gracilis</i>	0.73 \pm 0.02	1.04 \pm 0.03	0.47 \pm 0.08	0.26 \pm 0.02
Mix	<i>G. sulphuraria</i>	NG	NG	NG	NG
	<i>A. protothecoides</i>	1.94 \pm 0.04	1.59 \pm 0.03	1.72 \pm 0.03	0.43 \pm 0.02
	<i>E. gracilis</i>	0.87 \pm 0.01	0.52 \pm 0.01	0.27 \pm 0.02	0.28 \pm 0.04

9
 10 In addition, besides the expected depletion of acetate and glucose, a significant reduction of
 11 xylose concentration was also detected for *A. protothecoides* (from 46.3 to 21.9 mM carbon
 12 equivalent) despite no growth was stated in the presence of xylose alone (**Fig. 2C**). In the
 13 mixture, xylose assimilation started after one day of culture and accelerated until day 3, one
 14 day after reaching the stationary phase (**Fig. 3D**). This behavior with xylose in the presence of
 15 another carbon source has been previously documented in *A. protothecoides* and other
 16 microalgae [41,76,101,102]. As *A. protothecoides* was unable to consume xylose as the sole
 17 carbon source in our study, its uptake in the mix condition could be attributed to the induction
 18 of the glucose-induced hexose transporter [41]. Indeed, if xylose is assimilated through the
 19 same transporters as glucose but with lower affinity, it can explain why xylose uptake starts

1 when glucose is completely depleted (**Fig. 3D**). Consequently, rapid glucose depletion could
2 have stopped the glucose-induced xylose transport within the cell, explaining that only half
3 of the xylose was consumed by the end of the culture (24.5 mM). In a study of *A.*
4 *protothecoides* cultivation with glucose and reducing sugars (arabinose and xylose) provided
5 in nearly similar concentrations, but more elevated compared to this study (14-16 g L⁻¹ and 20
6 g L⁻¹, respectively, Chen et al. (2015)[101] reported a delayed pentose (xylose and arabinose)
7 assimilation compared to hexose assimilation, with pentose concentration in the medium
8 gradually decreasing after glucose/hexose depletion and after reaching the stationary phase.
9 Even if metabolized in specific context, the authors assessed that, during batch fermentation
10 in a 5-L stirred tank bioreactor, the global pentose consumption rate was approximately 10-
11 fold lower than the hexose consumption rate [101].

12 Using the formulas detailed in the **Material & Methods** section, the biomass yield on xylose
13 $Y_{x/xylose}$ was calculated based on the biomass yields on glucose and acetate as sole carbon
14 source, the amount of acetate, glucose and xylose consumed in the mix, and the maximal DW
15 concentration achieved in this condition ($X_{max_{mix}}$). Since biomass yields on glucose and
16 acetate as sole carbon source were 0.54 gDW g_{glucose}⁻¹ and 0.42 gDW g_{acetate}⁻¹, respectively,
17 the estimated biomass yield on xylose was 0.34 gDW g_{xylose}⁻¹, for *A. protothecoides* grown in
18 heterotrophy in a glucose-induced environment. Even if the deduced biomass yield is lower
19 compared to those calculated during the utilization of acetate and glucose, it is noteworthy
20 that xylose could be utilized to generate biomass for *A. protothecoides*, when grown in
21 heterotrophy in a glucose-supplemented environment. In addition, biomass yield on xylose is
22 practically never exposed for heterotrophic microalgae and the value calculated in this study
23 is close to those observed for bacterial and fungal wild-type species such as *E. coli* and *S.*
24 *cerevisiae* [44,103–105].

1 The mixed carbon source condition offered another non negligible advantage. Indeed, when
2 looking at (**Fig. 3B**), we can see that pH imbalance was reduced compared to the sole carbon
3 source conditions (glucose and acetate), enabling the complete utilization of acetate and
4 glucose introduced at the start of the culture. This is likely attributed to the balance between
5 glucose, ammonium, and acetate metabolisms, which lowers and raises the pH, respectively.
6 Consequently, this mixed condition appears to be the best optimal choice for *A.*
7 *protothecoides* compared to the other conditions biomass production, with the added benefit
8 of xylose valorization.

9

1 **Quantitative and qualitative analysis of the biomass composition of each**
2 **strain looking at the growth-effective carbon source.**

3 Samples were collected at the exponential and stationary phases for each strain in the
4 conditions in which growth was detected. In such case, the fatty acid, glycogen, paramylon or
5 starch, and protein and pigment contents were investigated.

6 **(i) Protein content**

7 In this study, regardless of the conditions or strains, the protein content ranged between 15%
8 and 35% of the total dry weight (**Fig. 4A**).

9 As shown in our previous work [20], *G. sulphuraria* grown on glucose exhibited a total protein
10 content of $32 \pm 3\%$ during exponential phase and $28 \pm 3\%$ during stationary phase. (**Fig. 4A**).

11 When grown on xylose, the microalgae showed a total protein content of $24 \pm 2\%$ and $30 \pm$
12 4% , during the exponential and the stationary phase, respectively (**Fig. 4A**). These results are
13 consistent with those reported for *G. sulphuraria* in heterotrophic conditions [10]. To our
14 knowledge, the value of 32% with glucose is the highest reported protein content similar to
15 [11].

16 Concerning *E. gracilis*, the protein content was $18 \pm 3\%$ and $34 \pm 7\%$ in the mix of all carbon
17 sources during the exponential and stationary phases, respectively, while it remained stable
18 at $28 \pm 2\%$ during growth with acetate only (**Fig. 4A**). These results align with literature when
19 *Euglena* is cultivated in the presence of glucose [13,24]. The protein content may vary from
20 10% to 52% depending on the nitrogen source, with ammonium sulfate being the most
21 effective [24]. The carbon-to-nitrogen (C/N) ratio also significantly impacts protein content
22 that is decreasing proportionally to the increase of the ratio. In the presence of acetate as the

1 sole carbon source, the C/N ratio remains constant (≥ 20) as both carbon and nitrogen sources
2 are consumed simultaneously until near depletion. However, when acetate is no longer
3 available in the mix, ammonium persists. Therefore, it is assumed that the C/N ratio decreases
4 as the stationary phase approaches, eventually leading to an increase in protein content.

5 The C/N ratio variations may also explain why *A. protothecoides* exhibited a protein content
6 ranging from $16 \pm 1\%$ in the presence of glucose to $31 \pm 2\%$ in the presence of acetate during
7 the exponential phase (**Fig. 4A**). Indeed, the C/N ratio is maintained higher in the presence of
8 glucose (around 35), since the sugar consumption led to rapid growth cessation due to pH
9 drop (**Fig. 3B**). While protein content doubles when stationary phase is reached in the
10 presence of glucose, an opposite behavior can be noticed in the presence of acetate (**Fig. 4A**).

11 This observation could be attributed to the rapid consumption of ammonium in the presence
12 of acetate, subsequently reducing the C/N ratio below 1. An intermediate protein content
13 ranged between $22 \pm 4\%$ and $30\% \pm 2\%$ was obtained under mix conditions regarding both
14 growth phases (**Fig. 4A**). Although some studies reported a low protein content for *Chlorella*
15 species such as *A. protothecoides* UTEX 25 in heterotrophy (4.3%) [18,106], they are typically
16 known to accumulate 25-50% protein in dry weight, even in heterotrophic conditions
17 [24,72,107].

18 In conclusion, heterotrophy is not an ideal growth cultivation for protein accumulation, and
19 the carbon source has a low impact on the total protein content under our conditions for any
20 of the strains. Protein content could be enhanced or reduced using different nitrogen sources
21 or by manipulating the C/N ratio at various points during cultivation.

22 (ii) Pigment content and profile

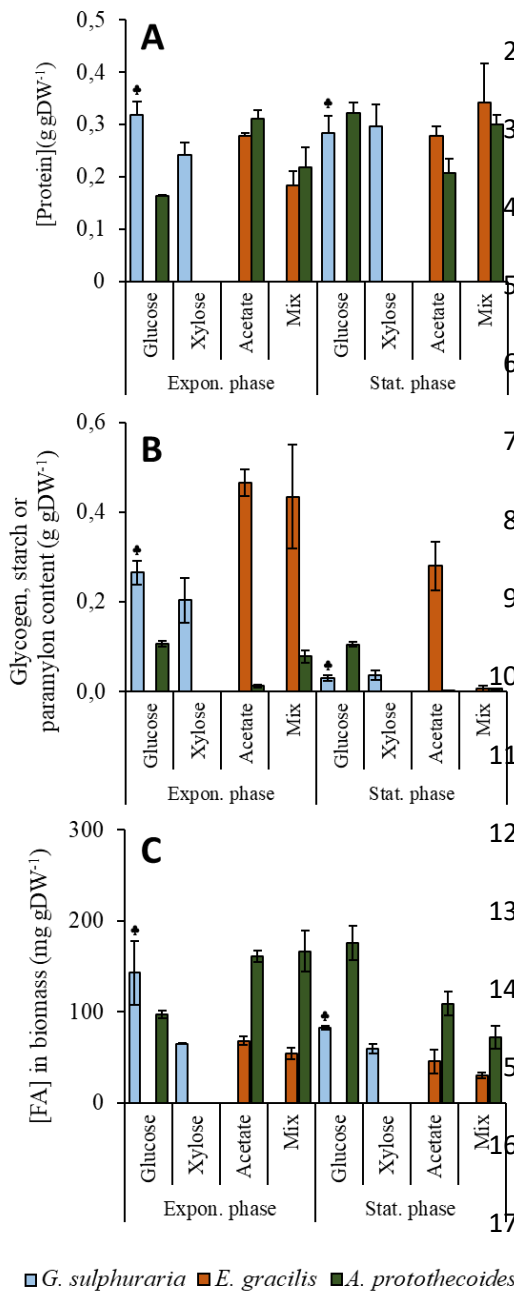


Figure 4: Total fatty acids, storage polysaccharides (glycogen, paramylon or starch), and protein content of *G. sulphuraria* (light blue bars), *E. gracilis* (orange bars), and *A. protothecoides* (dark green bars) cultures grown in heterotrophy in the presence of glucose, xylose, acetate, or a mix of the three carbon sources, during exponential or stationary phases. Bar charts (A) and (B) show the protein and storage polysaccharide content in biomass (expressed in g gDW⁻¹), respectively. Bar chart (C) shows the fatty acids content in biomass (expressed in mg gDW⁻¹). Data represent the mean of three independent biological replicates. Error bars represent the standard deviation of the mean (\pm SD). The clover symbol (\clubsuit) indicates values for *G. sulphuraria* grown on glucose from a previous study conducted in our laboratory [20].

1 It is widely documented that pigment content is
 2 low or even unmeasurable in heterotrophic
 3 conditions contrasting with phototrophic
 4 conditions because light exposure is essential for
 5 pigment synthesis. *G. sulphuraria* strain 074W
 6 exhibited dramatically diminished pigment
 7 content in the presence of glucose like previously
 8 reported in our lab [20] or xylose (Table S1).
 9 Consistent with these findings, *E. gracilis*
 10 exhibited extremely low pigment content and
 11 chlorophylls were completely absent, as
 12 reported in other studies conducted in
 13 heterotrophic conditions [24]. The pigment
 14 content of *A. protothecoides* was also very low
 15 during heterotrophic cultivation (Table S1), in
 16 line with previous reports [18,19,21]. Amongst
 17 the three carbon sources studied, glucose
 18 appears to have the most significant impact
 on photosynthetic pigment content. Specifically, when glucose is present, the total chlorophyll content is three times lower than in the presence of acetate during exponential phase. Conversely, when glucose is depleted in the stationary phase,

1 the chlorophyll levels are like those observed in the acetate condition, confirming the major
2 influence of glucose on pigment accumulation. The impact of glucose on photosynthetic
3 metabolism may involve different mechanisms that are not completely elucidated.
4 Transcriptional analysis of *G. sulphuraria* performed in our laboratory showed that glucose
5 have a negative effect on photosynthesis and pigment components compared to glycogen in
6 heterotrophy [20], or in the presence of light in mixotrophy [88]. In the green microalga
7 *Chromochloris zofingiensis* grown mixotrophically, exogenous glucose has an impact on gene
8 expression mediated by the hexokinase (HXK1) that subsequently represses photosynthetic-
9 related genes at a transcriptional level [108]. As discussed by the authors [108], the role of
10 the hexokinase on the photosynthetic machinery and pigments is unknown and could be
11 direct (initiating a signaling cascade) or indirect (involving metabolic intermediates).

12 **(ii) Glycogen, paramylon or starch content**

13 The glycogen content of *G. sulphuraria* cells grown in heterotrophy with glucose, as shown
14 previously [20], or xylose, is not significantly different and accounts for $26 \pm 3\%$ and $20 \pm 4\%$
15 of the total dry weight in the exponential phase (**Fig. 4B**). Similar biomass proportion was
16 observed in the presence of glycerol (20-36%) and glucose [17,109]. However, other results
17 have shown higher glycogen accumulation in almost similar conditions to those in the present
18 study, sometimes close to 70% of the total biomass [10,11].

19 In *E. gracilis*, paramylon content was around 45% in both acetate and mix conditions during
20 the exponential phase (**Fig. 4B**). Studies have demonstrated that paramylon content could
21 reach up to 80% of the total DW when cells are grown heterotrophically in the presence of
22 glucose instead of acetate [9,12,13]. Paramylon biosynthesis begins with the conversion of a
23 molecule of glucose to UDP-glucose [13,110]. Given our experimental conditions, which are

1 ATP-consuming since they require acetate conversion into glucose (see **Fig. 1** and [111], it is
2 understandable that the paramylon content would be reduced.

3 In *A. protothecoides*, the maximum starch content of $11 \pm 1\%$, is found under glucose
4 conditions, while around 1% was detected in the presence of acetate during the exponential
5 phase (**Fig. 4B**). In the mixed condition, starch content reached $8 \pm 1\%$, confirming that
6 glucose is more effective than acetate for starch production, as discussed above.

7 Overall, our results showed that glycogen, paramylon or starch contents were consistently
8 lower during the stationary phase (**Fig. 4B**). *G. sulphuraria* glycogen content exhibited a
9 significant decrease to 3-4% during the stationary phase. Similarly, *E. gracilis* paramylon
10 content dropped to nearly undetectable levels during the stationary phase in the mix
11 condition (**Fig. 4B**). Typically, microalgae utilize their storage polysaccharides to sustain
12 metabolic activity when carbon sources are depleted, thereby explaining the low content of
13 glycogen, paramylon or starch observed during the stationary phase, as long as other
14 nutrients such as phosphorous and nitrogen are available (**Fig. S1**). The remaining paramylon
15 content in *E. gracilis* in acetate (**Fig. 4B, Fig. S1**) could be due to the absence of ammonia
16 impeding paramylon catabolism, which was not the case for the mix condition (**Fig. 4B, Fig.**
17 **S1**). One exception noted is *A. protothecoides* in the presence of glucose, possibly due to
18 metabolic arrest triggered by low pH conditions.

19

Table 3: Fatty acids distribution in exponential and stationary phases when growth was observed in the presence of glucose, xylose, acetate or a mix of the three carbon sources for *G. sulphuraria*, *E. gracilis*, or *A. protothecoides*. SFA, saturated fatty acids; MUFA, mono-unsaturated fatty acids; PUFA, poly-unsaturated fatty acids. Data are expressed as a percentage of the FA species on the total FAs detected. Values represent the means \pm SD (n=3). ND: the FA species was not detected. The clover symbol (♣) indicates values for *G. sulphuraria* grown on glucose from a previous study conducted in our laboratory [20].

Fatty acid distribution in exponential phase

Fatty Acid	<i>G. sulphuraria</i>			<i>E. gracilis</i>			<i>A. protothecoides</i>			
	Glucose	Xylose	Acetate	Mix	Glucose	Acetate	Mix	Glucose	Acetate	Mix
C14:0	0.8 \pm 0.1 ♣	1.8 \pm 1.4	8.3 \pm 0.4	8.0 \pm 5.2	1.4 \pm 0.2	1.2 \pm 0.1	1.2 \pm 0.2			
C16:0	29.7 \pm 1.1 ♣	38.4 \pm 0.9	31.3 \pm 1.8	36.5 \pm 1.7	21.8 \pm 0.3	17.3 \pm 0.5	21.4 \pm 0.5			
C16:1	ND	ND	0.9 \pm 0.8	0.5 \pm 0.8	0.4 \pm 0.1	0.8 \pm ND	0.5 \pm ND			
C17:0	3.0 \pm 0.9 ♣	2.0 \pm 0.1	0.6 \pm 0.5	0.9 \pm 1.2	ND	ND	ND			
C17:1	ND	ND	ND	ND	ND	ND	ND			
C18:0	21.0 \pm 0.3 ♣	18.4 \pm 1.1	20.5 \pm 0.3	26.5 \pm 1.2	9.9 \pm 0.8	6.7 \pm 0.5	12.2 \pm 0.6			
C18:1n9t	1.2 \pm 1.1 ♣	ND	ND	ND	ND	ND	ND			
C18:1n9c	7.1 \pm 0.4 ♣	16.9 \pm 0.6	3.7 \pm 0.3	3.4 \pm 0.3	30.3 \pm 0.3	41.4 \pm 0.6	35.1 \pm 1.2			
C18:2n6c	13.6 \pm 1.1 ♣	14.5 \pm 1.3	0.5 \pm ND	1.4 \pm ND	27.1 \pm 0.8	27.3 \pm 0.5	24.0 \pm 0.7			
C18:3n3	19.1 \pm 1.3 ♣	3.4 \pm 0.2	0.7 \pm 0.6	ND	8.3 \pm 0.1	4.9 \pm 0.1	4.7 \pm 0.2			
C20:0	1.8 \pm 0.2 ♣	ND	0.5 \pm 0.5	ND	0.3 \pm ND	0.1 \pm 0.2	0.4 \pm ND			
C20:1n9	ND	ND	0.3 \pm 0.3	ND	ND	0.2 \pm 0.2	ND			
C20:2	ND	1.4 \pm 0.2	5.6 \pm 0.2	4.5 \pm ND	ND	ND	ND			
C20:3n6	ND	ND	1.3 \pm 0.1	ND	ND	ND	ND			
C20:4n6	ND	ND	8.0 \pm 0.5	4.5 \pm 0.3	ND	ND	ND			
C20:3n3	ND	ND	4.0 \pm 0.1	2.8 \pm 0.3	0.4 \pm ND	ND	0.5 \pm ND			
C22:0	ND	ND	2.1 \pm	ND	ND	ND	ND			
C22:1	ND	ND	3.8 \pm 0.2	2.7 \pm 0.1	ND	ND	ND			
C22:2	ND	ND	0.7 \pm 1.2	ND	ND	ND	ND			
C24:0	ND	ND	3.9 \pm 0.3	2.1 \pm 0.1	ND	ND	ND			
C24:1	ND	ND	ND	ND	ND	ND	ND			
C22:6n3	ND	ND	3.3 \pm 0.1	4.8 \pm 4.8	ND	ND	ND			
%SFA	59.0 \pm 0.6	62.9 \pm 0.8	67.2 \pm 1.1	75.4 \pm 4.7	33.4 \pm 0.9	25.3 \pm 1.0	35.2 \pm 1.3			
%MUFA	8.3 \pm 0.7	16.9 \pm 0.6	8.8 \pm 0.6	6.7 \pm 0.6	30.6 \pm 0.3	42.5 \pm 0.7	35.6 \pm 1.2			
%PUFA	32.7 \pm 0.5	20.2 \pm 0.1	27.8 \pm 1.3	20.7 \pm 4.2	36.0 \pm 1.2	32.2 \pm 0.5	29.2 \pm 0.9			

ND: The FA was not detected

Fatty acid distribution in stationary phase

Fatty Acid	<i>G. sulphuraria</i>			<i>E. gracilis</i>			<i>A. protothecoides</i>			
	Glucose	Xylose	Acetate	Mix	Glucose	Acetate	Mix	Glucose	Acetate	Mix
C14:0	0.9 \pm 0.0 ♣	0.8 \pm 0.2	6.2 \pm 1.7	3.0 \pm 1.6	1.4 \pm 0.0	0.8 \pm 0.2	0.9 \pm 0.1			
C16:0	29.2 \pm 0.4 ♣	34.3 \pm 0.3	26.5 \pm 3.9	39.1 \pm 1.6	17.2 \pm 0.4	12.9 \pm 0.1	21.0 \pm 0.3			
C16:1	0.4 \pm 0.3 ♣	ND	1.1 \pm 0.1	ND	0.5 \pm 0.0	1.3 \pm 0.1	0.6 \pm 0.0			
C17:0	3.0 \pm 0.1 ♣	2.9 \pm 0.1	0.7 \pm 0.2	ND	ND	ND	ND			
C17:1	1.7 \pm 0.0 ♣	0.9 \pm 0.0	ND	ND	ND	ND	ND			
C18:0	7.6 \pm 0.3 ♣	11.7 \pm 0.0	18.9 \pm 2.9	31.3 \pm 2.6	5.2 \pm 0.3	3.1 \pm 0.1	8.7 \pm 0.3			
C18:1n9t	0.5 \pm 0.1 ♣	ND	ND	ND	ND	ND	ND			
C18:1n9c	15.6 \pm 0.2 ♣	17.8 \pm 0.0	3.9 \pm 0.1	2.9 \pm 0.0	38.7 \pm 0.7	43.0 \pm 0.4	20.4 \pm 0.8			
C18:2n6c	27.0 \pm 0.7 ♣	21.6 \pm 0.4	0.8 \pm 0.1	1.4 \pm 0.2	28.2 \pm 0.3	33.3 \pm 0.3	38.0 \pm 0.3			
C18:3n3	5.6 \pm 0.2 ♣	4.1 \pm 0.6	1.7 \pm 0.1	ND	8.1 \pm 0.2	4.9 \pm 0.3	10.0 \pm 0.5			
C20:0	0.6 \pm 0.1 ♣	ND	ND	ND	0.3 \pm 0.0	0.2 \pm 0.0	0.2 \pm 0.0			
C20:1n9	0.3 \pm 0.1 ♣	0.5 \pm 0.0	0.2 \pm 0.3	ND	0.2 \pm 0.2	0.2 \pm 0.1	ND			
C20:2	2.4 \pm 0.0 ♣	1.6 \pm 0.0	7.1 \pm 0.7	4.4 \pm 0.7	ND	ND	ND			
C20:3n6	ND	ND	1.0 \pm 0.3	ND	ND	ND	ND			
C20:4n6	ND	ND	10.4 \pm 1.9	4.1 \pm 0.3	ND	ND	ND			
C20:3n3	ND	ND	5.0 \pm 0.8	2.3 \pm 0.5	0.2 \pm 0.0	ND	0.4 \pm 0.0			
C22:0	ND	ND	1.7 \pm 1.0	1.3 \pm 1.8	ND	ND	ND			
C22:1	ND	ND	4.4 \pm 0.6	2.3 \pm 0.2	ND	ND	ND			
C22:2	ND	ND	ND	ND	ND	ND	ND			
C24:0	ND	ND	5.7 \pm 1.1	1.9 \pm 0.5	ND	ND	ND			
C24:1	ND	ND	ND	ND	ND	ND	ND			
C22:6n3	ND	ND	4.7 \pm 0.6	6.2 \pm 5.4	ND	ND	ND			
%SFA	45.8 \pm 0.7	53.6 \pm 0.9	59.7 \pm 4.2	76.5 \pm 4.9	24.1 \pm 0.7	17.1 \pm 0.3	30.8 \pm 0.7			
%MUFA	19.2 \pm 0.4	19.1 \pm 0.1	9.5 \pm 0.8	5.2 \pm 0.2	39.4 \pm 0.7	44.6 \pm 0.5	20.9 \pm 0.8			
%PUFA	34.9 \pm 0.5	27.2 \pm 0.9	35.2 \pm 4.1	20.6 \pm 4.9	36.5 \pm 0.1	38.3 \pm 0.5	48.3 \pm 0.7			

(iv) Fatty acid (FA) content and profile

The FA content and profile of *G. sulphuraria* in the presence of glucose was reported in a previous study [20]. The total FA content in glucose was $14 \pm 4\%$ while it has been shown to be $6 \pm 1\%$ in the presence of xylose in the present work (**Fig. 4C**). Unlike glycogen content, FA content remained stable during the stationary phase, (**Fig. 4C**). These results are in line with other studies where the total FA content observed in the presence of various carbon sources never exceeds 6% and do not decrease (or even increase) when cells reach the stationary phase [52,112]. This behavior suggests that glycogen is more likely utilized by the cell than FAs as a carbon source during carbon starvation. Additionally, *G. sulphuraria* has high proportions of SFAs in both conditions and growth phases, which is uncommon for red algae [113]. SFAs distribution reached up to 60% of the total FAs during exponential phase, with predominant C16:0 and C18:0 (up to $38 \pm 1\%$ as C16:0 in the presence of xylose), while polyunsaturated fatty acids (PUFAs) accounted for $33 \pm 1\%$ and $20 \pm 1\%$ in the glucose and xylose conditions, respectively. At the end of the culture, unsaturated fatty acid content is slightly elevated, but SFAs remain dominant with $46 \pm 1\%$ in the presence of glucose and $54 \pm 1\%$ in the presence of xylose (**Table 3**). [52] reported very similar results to the present study. In summary, even though *G. sulphuraria* total FA content is low compared to oleaginous microalgae, it is promising for the valorization of xylose-rich hemicellulose-containing biomass in the context of biofuel production because of its high biomass productivity using xylose and high levels of SFAs. The observed *G. sulphuraria* FA distribution could be suitable for conversion into medium-chain fuels such as biokerosene that allow the presence of some unsaturation, lowering its melting point and thus increasing the cold flow properties of the fuel [114].

E. gracilis exhibited a total FA content during the exponential phase of only $7 \pm 1\%$ in the acetate condition and $5 \pm 1\%$ with a mix of all three carbon sources. These percentages decreased to $5 \pm 1\%$ and $3 \pm 1\%$, upon reaching the stationary phase (**Fig. 4C**). FA distribution shows a high yield of SFAs in both growth conditions, reaching up to $75 \pm 1\%$ in the presence of mixed carbon sources with no distinction in the monitored growth phase (**Table 3**). These observations are in agreement with those previously published [57]. The predominant SFAs found were C16:0 (31-37%), C18:0 (21-27%), and C14:0 (8%), depending on the growth condition.

A. protothecoides generally exhibited higher FA content than the two other species studied, with $16 \pm 1\%$ and $17 \pm 2\%$ in the acetate and mix conditions, respectively. The assimilation of acetate could lead to better FA accumulation than glucose in the mix since acetate is rapidly converted into acetyl-CoA after its entry into the cytosol by the acetyl-CoA synthase, the key molecule to start FA biosynthesis, as in [78,115,116]. When reaching the stationary phase, the total FA content decreased in the acetate and mix conditions, to $11 \pm 1\%$ and $7 \pm 1\%$, respectively (**Fig. 4C**). The decrease of FA in the stationary phase could be explained by their utilization when the carbon source and the starch reserves are depleted, while other nutrients remain as mentioned above (**Fig. S1**). In contrast, the same levels of FAs ($18 \pm 2\%$) were found once the stationary phase was reached in the presence of glucose as during the exponential phase for the acetate and mix conditions (**Fig. 4C**), possibly due to their accumulation before cell death caused by the prementioned low pH stress. Regardless of the growth phase, FA content is barely affected by the carbon source, as long as the cells can assimilate it. Even if no studies were conducted in the presence of a mix the three carbon sources, similar observations have been reported before for *A. protothecoides* grown heterotrophically with a total lipid content of approximately 20% in the presence of either glucose, glycerol, or

acetate [115]. In our study, we observed that FAs are almost equally distributed among SFAs, mono-unsaturated fatty acids (MUFAs), and in all conditions during the exponential phase (ranging from 25% to 42% each) (**Table 3**). As the stationary phase of growth is reached, the proportion of SFAs decreases in the glucose and acetate conditions, increasing the amount of MUFAs. However, in the mixed condition, the end of the culture is marked by a decrease in MUFAs and an increase in PUFAs, which are less suitable for biofuel production (**Table 3**). Irrespectively of the growth conditions, the main represented SFAs are palmitic and stearic acids (C:16 and C:18, respectively), while oleic acid (C18:1) is the only representative of MUFAs, accounting for 30-43% of the total FAs in both growth phases. The primary PUFA produced is linoleic acid (C18:2 ω -6), accounting for 24-27% in the exponential phase and 28-38% in the stationary phase, comparable to levels reported in other studies on heterotrophically grown *A. protothecoides* [29,117,118]. In summary, *A. protothecoides*, widely studied for lipid production in heterotrophy, shows a lipid content comparable to other oleaginous microalgae in all conditions. Since high levels of SFAs and MUFAs could be observed together with xylose assimilation in the mixed condition, it appears to be a good candidate for hemicellulose valorization in the context of biofuel production.

Conclusion

The present study highlights the potential of three microalgal species—*A. protothecoides*, *G. sulphuraria*, and *E. gracilis*—for biomass valorization using hemicellulose-containing carbon sources through heterotrophic cultivation. Each species demonstrated unique growth characteristics and metabolic capabilities, offering distinct advantages for specific applications. *G. sulphuraria* showed notable biomass yields, particularly with xylose as the sole carbon source, and produced high levels of SFAs, glycogen, and proteins. *E. gracilis*, although limited by its inability to assimilate glucose or xylose, efficiently utilized acetate and stored a significant amount of carbohydrates as paramylon, which can be converted into wax esters under anaerobic conditions. *A. protothecoides* emerged as the most versatile species, capable of efficient growth when all three carbon sources (acetate, glucose, and xylose) were combined. The high specific growth rate, remarkable FA content (mostly SFAs and MUFAs) in combination with low starch and pigment content, make this alga a promising candidate for biofuel production from hemicellulose hydrolysate. In addition, the ability of *A. protothecoides* to maintain pH balance in mixed carbon source media further underscores its suitability for industrial applications. Future research should focus on the scalability of *A. protothecoides* cultivation using actual hardwood hemicellulose hydrolysate to validate its potential in biofuel production. Overall, the findings from this study provide a solid foundation for the development of sustainable and efficient microalgal-based bioprocesses for hemicellulose valorization.

References

- [1] M. Gouda, M.A. Tadda, Y. Zhao, F. Farmanullah, B. Chu, X. Li, Y. He, Microalgae Bioactive Carbohydrates as a Novel Sustainable and Eco-Friendly Source of Prebiotics: Emerging Health Functionality and Recent Technologies for Extraction and Detection, *Front. Nutr.* 9 (2022) 806692. <https://doi.org/10.3389/fnut.2022.806692>.
- [2] Y. Qiao, F. Yang, T. Xie, Z. Du, D. Zhong, Y. Qi, Y. Li, W. Li, Z. Lu, J. Rao, Y. Sun, M. Zhou, Engineered algae: A novel oxygen-generating system for effective treatment of hypoxic cancer, *Sci. Adv.* 6 (2020) eaba5996. <https://doi.org/10.1126/sciadv.aba5996>.
- [3] R. Ravindran, G. Rajauria, Carbohydrates derived from microalgae in the food industry, in: *Cult. Microalgae Food Ind.*, Elsevier, 2021: pp. 127–146. <https://doi.org/10.1016/B978-0-12-821080-2.00007-1>.
- [4] T. Ghidossi, I. Marison, R. Devery, D. Gaffney, C. Forde, Characterization and Optimization of a Fermentation Process for the Production of High Cell Densities and Lipids Using Heterotrophic Cultivation of *Chlorella protothecoides*, *Ind. Biotechnol.* 13 (2017) 253–259. <https://doi.org/10.1089/ind.2017.0007>.
- [5] L. Rodolfi, G. Chini Zittelli, N. Bassi, G. Padovani, N. Biondi, G. Bonini, M.R. Tredici, Microalgae for oil: Strain selection, induction of lipid synthesis and outdoor mass cultivation in a low-cost photobioreactor, *Biotechnol. Bioeng.* 102 (2009) 100–112. <https://doi.org/10.1002/bit.22033>.
- [6] A.K. Sharma, P.K. Sahoo, S. Singhal, A. Patel, Impact of various media and organic carbon sources on biofuel production potential from *Chlorella* spp., *3 Biotech* 6 (2016) 116. <https://doi.org/10.1007/s13205-016-0434-6>.
- [7] H. Xu, X. Miao, Q. Wu, High quality biodiesel production from a microalga *Chlorella protothecoides* by heterotrophic growth in fermenters, *J. Biotechnol.* 126 (2006) 499–507. <https://doi.org/10.1016/j.jbiotec.2006.05.002>.
- [8] R. Barone, L. De Napoli, L. Mayol, M. Paolucci, M.G. Volpe, L. D’Elia, A. Pollio, M. Guida, E. Gambino, F. Carraturo, R. Marra, F. Vinale, S.L. Woo, M. Lorito, Autotrophic and Heterotrophic Growth Conditions Modify Biomolecule Production in the Microalga *Galdieria sulphuraria* (Cyanidiophyceae, Rhodophyta), *Mar. Drugs* 18 (2020) 169. <https://doi.org/10.3390/md18030169>.
- [9] A. Gissibl, A. Sun, A. Care, H. Nevalainen, A. Sunna, Bioproducts From *Euglena gracilis*: Synthesis and Applications, *Front. Bioeng. Biotechnol.* 7 (2019) 108. <https://doi.org/10.3389/fbioe.2019.00108>.
- [10] G. Graziani, S. Schiavo, M.A. Nicolai, S. Buono, V. Fogliano, G. Pinto, A. Pollio, Microalgae as human food: chemical and nutritional characteristics of the thermo-acidophilic microalga *Galdieria sulphuraria*, *Food Funct* 4 (2013) 144–152. <https://doi.org/10.1039/C2FO30198A>.
- [11] M. Massa, S. Buono, A.L. Langellotti, A. Martello, G.L. Russo, D.A. Troise, R. Sacchi, P. Vitaglione, V. Fogliano, Biochemical composition and in vitro digestibility of *Galdieria sulphuraria* grown on spent cherry-brine liquid, *New Biotechnol.* 53 (2019) 9–15. <https://doi.org/10.1016/j.nbt.2019.06.003>.
- [12] A. Sun, M.T. Hasan, G. Hobba, H. Nevalainen, J. Te’o, Comparative assessment of the *Euglena gracilis* var. *saccharophila* variant strain as a producer of the β -1,3-glucan paramylon under varying light conditions, *J. Phycol.* 54 (2018) 529–538. <https://doi.org/10.1111/jpy.12758>.
- [13] M. Wu, H. Qin, J. Deng, Y. Liu, A. Lei, H. Zhu, Z. Hu, J. Wang, A new pilot-scale fermentation mode enhances *Euglena gracilis* biomass and paramylon (β -1,3-glucan) production, *J. Clean. Prod.* 321 (2021) 128996. <https://doi.org/10.1016/j.jclepro.2021.128996>.
- [14] S. Koritala, Microbiological synthesis of wax esters by *euglena gracilis*, *J. Am. Oil Chem. Soc.* 66 (1989) 133–134. <https://doi.org/10.1007/BF02661801>.

- [15] X. Miao, Q. Wu, High yield bio-oil production from fast pyrolysis by metabolic controlling of *Chlorella protothecoides*, *J. Biotechnol.* 110 (2004) 85–93. <https://doi.org/10.1016/j.jbiotec.2004.01.013>.
- [16] M.A. Mohammad Mirzaie, M. Kalbasi, S.M. Mousavi, B. Ghobadian, Investigation of mixotrophic, heterotrophic, and autotrophic growth of *Chlorella vulgaris* under agricultural waste medium, *Prep. Biochem. Biotechnol.* 46 (2016) 150–156. <https://doi.org/10.1080/10826068.2014.995812>.
- [17] T. Sakurai, M. Aoki, X. Ju, T. Ueda, Y. Nakamura, S. Fujiwara, T. Umemura, M. Tsuzuki, A. Minoda, Profiling of lipid and glycogen accumulations under different growth conditions in the sulfotolerant red alga *Galdieria sulphuraria*, *Bioresour. Technol.* 200 (2016) 861–866. <https://doi.org/10.1016/j.biortech.2015.11.014>.
- [18] C.D. Lane, D.A. Coury, F.C.T. Allnut, Composition and Potential Products from *Auxenochlorella protothecoides*, *Chlorella sorokiniana* and *Chlorella vulgaris*, *Ind. Biotechnol.* 13 (2017) 270–276. <https://doi.org/10.1089/ind.2017.0015>.
- [19] G. Markou, A. Diamantis, E. Korozi, V. Tsagou, I. Kefalogianni, I. Chatzipavlidis, Effects of Monochromatic Illumination with LEDs Lights on the Growth and Photosynthetic Performance of *Auxenochlorella protothecoides* in Photo- and Mixotrophic Conditions, *Plants* 10 (2021) 799. <https://doi.org/10.3390/plants10040799>.
- [20] P. Perez Saura, M. Chabi, A. Corato, P. Cardol, C. Remacle, Cell adaptation of the extremophilic red microalga *Galdieria sulphuraria* to the availability of carbon sources, *Front. Plant Sci.* 13 (2022) 978246. <https://doi.org/10.3389/fpls.2022.978246>.
- [21] Y. Xiao, X. He, Q. Ma, Y. Lu, F. Bai, J. Dai, Q. Wu, Photosynthetic Accumulation of Lutein in *Auxenochlorella protothecoides* after Heterotrophic Growth, *Mar. Drugs* 16 (2018) 283. <https://doi.org/10.3390/md16080283>.
- [22] F. Abiusi, P. Moñino Fernández, S. Canziani, M. Janssen, R.H. Wijffels, M. Barbosa, Mixotrophic cultivation of *Galdieria sulphuraria* for C-phycoerythrin and protein production, *Algal Res.* 61 (2022) 102603. <https://doi.org/10.1016/j.algal.2021.102603>.
- [23] S.R. Chae, E.J. Hwang, H.S. Shin, Single cell protein production of *Euglena gracilis* and carbon dioxide fixation in an innovative photo-bioreactor, *Bioresour. Technol.* 97 (2006) 322–329. <https://doi.org/10.1016/j.biortech.2005.02.037>.
- [24] W. Xie, X. Li, H. Xu, F. Chen, K.-W. Cheng, H. Liu, B. Liu, Optimization of Heterotrophic Culture Conditions for the Microalgae *Euglena gracilis* to Produce Proteins, *Mar. Drugs* 21 (2023) 519. <https://doi.org/10.3390/md21100519>.
- [25] H. Li, Z. Liu, Y. Zhang, B. Li, H. Lu, N. Duan, M. Liu, Z. Zhu, B. Si, Conversion efficiency and oil quality of low-lipid high-protein and high-lipid low-protein microalgae via hydrothermal liquefaction, *Bioresour. Technol.* 154 (2014) 322–329. <https://doi.org/10.1016/j.biortech.2013.12.074>.
- [26] L. Matricon, A. Roubaud, G. Haarlemmer, C. Geantet, The challenge of nitrogen compounds in hydrothermal liquefaction of algae, *J. Supercrit. Fluids* 196 (2023) 105867. <https://doi.org/10.1016/j.supflu.2023.105867>.
- [27] F. Obeid, T. Chu Van, R. Brown, T. Rainey, Nitrogen and sulphur in algal biocrude: A review of the HTL process, upgrading, engine performance and emissions, *Energy Convers. Manag.* 181 (2019) 105–119. <https://doi.org/10.1016/j.enconman.2018.11.054>.
- [28] R. Ranjith Kumar, P. Hanumantha Rao, M. Arumugam, Lipid Extraction Methods from Microalgae: A Comprehensive Review, *Front. Energy Res.* 2 (2015). <https://doi.org/10.3389/fenrg.2014.00061>.
- [29] A. Patel, L. Matsakas, U. Rova, P. Christakopoulos, Heterotrophic cultivation of *Auxenochlorella protothecoides* using forest biomass as a feedstock for sustainable biodiesel production, *Biotechnol. Biofuels* 11 (2018) 169. <https://doi.org/10.1186/s13068-018-1173-1>.
- [30] F.V.-L. Portillo, E. Sierra-Ibarra, R. Vera-Estrella, S. Revah, O.T. Ramírez, L. Caspeta, A. Martínez, Growth and phycocyanin production with *Galdieria sulphuraria* UTEX 2919 using

- xylose, glucose, and corn stover hydrolysates under heterotrophy and mixotrophy, *Algal Res.* 65 (2022) 102752. <https://doi.org/10.1016/j.algal.2022.102752>.
- [31] T.-Y. Zhang, Y.-H. Wu, J.-H. Wang, X.-X. Wang, V.M. Deantes-Espinosa, G.-H. Dao, X. Tong, H.-Y. Hu, Heterotrophic cultivation of microalgae in straw lignocellulose hydrolysate for production of high-value biomass rich in polyunsaturated fatty acids (PUFA), *Chem. Eng. J.* 367 (2019) 37–44. <https://doi.org/10.1016/j.cej.2019.02.049>.
- [32] A. Ebringerová, Structural Diversity and Application Potential of Hemicelluloses, *Macromol. Symp.* 232 (2005) 1–12. <https://doi.org/10.1002/masy.200551401>.
- [33] A. Aho, M. Alvear, J. Ahola, J. Kangas, J. Tanskanen, I. Simakova, J.L. Santos, K. Eränen, T. Salmi, D.Y. Murzin, H. Grénman, Aqueous phase reforming of birch and pine hemicellulose hydrolysates, *Bioresour. Technol.* 348 (2022) 126809. <https://doi.org/10.1016/j.biortech.2022.126809>.
- [34] K. Miazek, C. Remacle, A. Richel, D. Goffin, Beech wood *Fagus sylvatica* dilute-acid hydrolysate as a feedstock to support *Chlorella sorokiniana* biomass, fatty acid and pigment production, *Bioresour. Technol.* 230 (2017) 122–131. <https://doi.org/10.1016/j.biortech.2017.01.034>.
- [35] J.S. Van Dyk, B.I. Pletschke, A review of lignocellulose bioconversion using enzymatic hydrolysis and synergistic cooperation between enzymes—Factors affecting enzymes, conversion and synergy, *Biotechnol. Adv.* 30 (2012) 1458–1480. <https://doi.org/10.1016/j.biotechadv.2012.03.002>.
- [36] W. Tanner, The *Chlorella* hexose/H⁺-symporters, in: *Int. Rev. Cytol.*, Elsevier, 2000: pp. 101–141. [https://doi.org/10.1016/S0074-7696\(00\)00003-6](https://doi.org/10.1016/S0074-7696(00)00003-6).
- [37] O. Perez-Garcia, F.M.E. Escalante, L.E. de-Bashan, Y. Bashan, Heterotrophic cultures of microalgae: Metabolism and potential products, *Water Res.* 45 (2011) 11–36. <https://doi.org/10.1016/j.watres.2010.08.037>.
- [38] W. Ran, H. Wang, Y. Liu, M. Qi, Q. Xiang, C. Yao, Y. Zhang, X. Lan, Storage of starch and lipids in microalgae: Biosynthesis and manipulation by nutrients, *Bioresour. Technol.* 291 (2019) 121894. <https://doi.org/10.1016/j.biortech.2019.121894>.
- [39] H. Wang, Y. Zhang, W. Zhou, L. Noppol, T. Liu, Mechanism and enhancement of lipid accumulation in filamentous oleaginous microalgae *Tribonema minus* under heterotrophic condition, *Biotechnol. Biofuels* 11 (2018) 328. <https://doi.org/10.1186/s13068-018-1329-z>.
- [40] G. Proietti Tocca, V. Agostino, B. Menin, T. Tommasi, D. Fino, F. Di Caprio, Mixotrophic and heterotrophic growth of microalgae using acetate from different production processes, *Rev. Environ. Sci. Biotechnol.* 23 (2024) 93–132. <https://doi.org/10.1007/s11157-024-09682-7>.
- [41] Y. Zheng, X. Yu, T. Li, X. Xiong, S. Chen, Induction of D-xylose uptake and expression of NAD(P)H-linked xylose reductase and NADP⁺-linked xylitol dehydrogenase in the oleaginous microalga *Chlorella sorokiniana*, (2014).
- [42] H. Alper, G. Stephanopoulos, Engineering for biofuels: exploiting innate microbial capacity or importing biosynthetic potential?, *Nat. Rev. Microbiol.* 7 (2009) 715–723. <https://doi.org/10.1038/nrmicro2186>.
- [43] G.B. Leite, K. Paranjape, P.C. Hallenbeck, Breakfast of champions: Fast lipid accumulation by cultures of *Chlorella* and *Scenedesmus* induced by xylose, *Algal Res.* 16 (2016) 338–348. <https://doi.org/10.1016/j.algal.2016.03.041>.
- [44] M. Song, H. Pei, The growth and lipid accumulation of *Scenedesmus quadricauda* during batch mixotrophic/heterotrophic cultivation using xylose as a carbon source, *Bioresour. Technol.* 263 (2018) 525–531. <https://doi.org/10.1016/j.biortech.2018.05.020>.
- [45] L.C. Krämer, D. Wasser, F. Haitz, B. Sabel, C. Büchel, Heterologous expression of HUP1 glucose transporter enables low-light mediated growth on glucose in *Phaeodactylum tricorutum*, *Algal Res.* 64 (2022) 102719. <https://doi.org/10.1016/j.algal.2022.102719>.
- [46] W. Zhang, W. Zhou, S. Jiang, Y. Wang, L. Chen, G. Yang, T. Liu, Heterotrophic modification of *Phaeodactylum tricorutum* Bohlin, *Algal Res.* 72 (2023) 103137. <https://doi.org/10.1016/j.algal.2023.103137>.

- [47] A. Doebbe, J. Rupprecht, J. Beckmann, J.H. Mussnug, A. Hallmann, B. Hankamer, O. Kruse, Functional integration of the HUP1 hexose symporter gene into the genome of *C. reinhardtii*: Impacts on biological H₂ production, *J. Biotechnol.* 131 (2007) 27–33. <https://doi.org/10.1016/j.jbiotec.2007.05.017>.
- [48] L.A. Zaslavskaja, J.C. Lippmeier, C. Shih, D. Ehrhardt, A.R. Grossman, K.E. Apt, Trophic Conversion of an Obligate Photoautotrophic Organism Through Metabolic Engineering, *Science* 292 (2001) 2073–2075. <https://doi.org/10.1126/science.160015>.
- [49] W. Gross, C. Schnarrenberger, Heterotrophic Growth of Two Strains of the Acido-Thermophilic Red Alga *Galdieria sulphuraria*, *Plant Cell Physiol.* 36 (1995) 633–638. <https://doi.org/10.1093/oxfordjournals.pcp.a078803>.
- [50] R.A. Schmidt, M.G. Wiebe, N.T. Eriksen, Heterotrophic high cell-density fed-batch cultures of the phycocyanin-producing red alga *Galdieria sulphuraria*, *Biotechnol. Bioeng.* 90 (2005) 77–84. <https://doi.org/10.1002/bit.20417>.
- [51] E.G. Giakoumis, A statistical investigation of biodiesel physical and chemical properties, and their correlation with the degree of unsaturation, *Renew. Energy* 50 (2013) 858–878. <https://doi.org/10.1016/j.renene.2012.07.040>.
- [52] G. López, C. Yate, F.A. Ramos, M.P. Cala, S. Restrepo, S. Baena, Production of Polyunsaturated Fatty Acids and Lipids from Autotrophic, Mixotrophic and Heterotrophic cultivation of *Galdieria* sp. strain USBA-GBX-832, *Sci. Rep.* 9 (2019) 10791. <https://doi.org/10.1038/s41598-019-46645-3>.
- [53] M. Martinez-Garcia, A. Kormpa, M.J.E.C. van der Maarel, The glycogen of *Galdieria sulphuraria* as alternative to starch for the production of slowly digestible and resistant glucose polymers, *Carbohydr. Polym.* 169 (2017) 75–82. <https://doi.org/10.1016/j.carbpol.2017.04.004>.
- [54] N. Pade, N. Linka, W. Ruth, A.P.M. Weber, M. Hagemann, Floridoside and isofloridoside are synthesized by trehalose 6-phosphate synthase-like enzymes in the red alga *Galdieria sulphuraria*, *New Phytol.* 205 (2015) 1227–1238. <https://doi.org/10.1111/nph.13108>.
- [55] Y. Huang, X. Wan, Z. Zhao, H. Liu, Y. Wen, W. Wu, X. Ge, C. Zhao, Metabolomic analysis and pathway profiling of paramylon production in *Euglena gracilis* grown on different carbon sources, *Int. J. Biol. Macromol.* 246 (2023) 125661. <https://doi.org/10.1016/j.ijbiomac.2023.125661>.
- [56] R. Russo, L. Barsanti, V. Evangelista, A.M. Frassanito, V. Longo, L. Pucci, G. Penno, P. Gualtieri, *Euglena gracilis* paramylon activates human lymphocytes by upregulating pro-inflammatory factors, *Food Sci. Nutr.* 5 (2017) 205–214. <https://doi.org/10.1002/fsn3.383>.
- [57] J.-M. Jung, J.Y. Kim, S. Jung, Y.-E. Choi, E.E. Kwon, Quantitative study on lipid productivity of *Euglena gracilis* and its biodiesel production according to the cultivation conditions, *J. Clean. Prod.* 291 (2021) 125218. <https://doi.org/10.1016/j.jclepro.2020.125218>.
- [58] M. Nakazawa, H. Andoh, K. Koyama, Y. Watanabe, T. Nakai, M. Ueda, T. Sakamoto, H. Inui, Y. Nakano, K. Miyatake, Alteration of Wax Ester Content and Composition in *Euglena gracilis* with Gene Silencing of 3-ketoacyl-CoA Thiolase Isozymes, *Lipids* 50 (2015) 483–492. <https://doi.org/10.1007/s11745-015-4010-3>.
- [59] Y.-H. Chen, T.H. Walker, Biomass and lipid production of heterotrophic microalgae *Chlorella protothecoides* by using biodiesel-derived crude glycerol, *Biotechnol. Lett.* 33 (2011) 1973–1983. <https://doi.org/10.1007/s10529-011-0672-y>.
- [60] J. Wang, W.R. Curtis, Proton stoichiometric imbalance during algae photosynthetic growth on various nitrogen sources: toward metabolic pH control, *J. Appl. Phycol.* 28 (2016) 43–52. <https://doi.org/10.1007/s10811-015-0551-3>.
- [61] Z. Zhao, M. Xian, M. Liu, G. Zhao, Biochemical routes for uptake and conversion of xylose by microorganisms, *Biotechnol. Biofuels* 13 (2020) 21. <https://doi.org/10.1186/s13068-020-1662-x>.

- [62] M.B. Allen, Studies with cyanidium caldarium, an anomalously pigmented chlorophyte, Arch. Mikrobiol. 32 (1959) 270–277. <https://doi.org/10.1007/BF00409348>.
- [63] D.S. Gorman, R.P. Levine, Cytochrome f and plastocyanin: their sequence in the photosynthetic electron transport chain of Chlamydomonas reinhardi., Proc. Natl. Acad. Sci. 54 (1965) 1665–1669. <https://doi.org/10.1073/pnas.54.6.1665>.
- [64] S.H. Hutner, A.C. Zahalsky, S. Aaronson, H. Baker, O. Frank, Chapter 8 Culture Media for Euglena gracilis, in: Methods Cell Biol., Elsevier, 1966: pp. 217–228. [https://doi.org/10.1016/S0091-679X\(08\)62140-8](https://doi.org/10.1016/S0091-679X(08)62140-8).
- [65] J. Murphy, J.P. Riley, A modified single solution method for the determination of phosphate in natural waters, Anal. Chim. Acta 27 (1962) 31–36. [https://doi.org/10.1016/S0003-2670\(00\)88444-5](https://doi.org/10.1016/S0003-2670(00)88444-5).
- [66] T.A. Kursar, J. Van Der Meer, R.S. Alberte, Light-Harvesting System of the Red Alga Gracilaria tikvahiae: I. Biochemical Analyses of Pigment Mutations, Plant Physiol. 73 (1983) 353–360. <https://doi.org/10.1104/pp.73.2.353>.
- [67] O.H. Lowry, N.J. Rosebrough, A.L. Farr, R.J. Randall, Protein measurement with the Folin phenol reagent, J. Biol. Chem. 193 (1951) 265–275.
- [68] S.S. Nielsen, Phenol-Sulfuric Acid Method for Total Carbohydrates, in: S.S. Nielsen (Ed.), Food Anal. Lab. Man., Springer US, Boston, MA, 2010: pp. 47–53. https://doi.org/10.1007/978-1-4419-1463-7_6.
- [69] A. Corato, T.T. Le, D. Baurain, P. Jacques, C. Remacle, F. Franck, A Fast-Growing Oleaginous Strain of Coelastrella Capable of Astaxanthin and Canthaxanthin Accumulation in Phototrophy and Heterotrophy, Life 12 (2022) 334. <https://doi.org/10.3390/life12030334>.
- [70] R.C. Bates, R.E. Hurlbert, The Effect of Acetate on Euglena gracilis var. bacillaris as a Function of Environmental Conditions, J. Protozool. 17 (1970) 134–138. <https://doi.org/10.1111/j.1550-7408.1970.tb05172.x>.
- [71] J.R. Cook, B. Heinrich, Glucose vs. Acetate Metabolism in Euglena *, J. Protozool. 12 (1965) 581–584. <https://doi.org/10.1111/j.1550-7408.1965.tb03258.x>.
- [72] J.-P. Schwarzhans, D. Cholewa, P. Grimm, U. Beshay, J.-M. Risse, K. Friehs, E. Flaschel, Dependency of the fatty acid composition of Euglena gracilis on growth phase and culture conditions, J. Appl. Phycol. 27 (2015) 1389–1399. <https://doi.org/10.1007/s10811-014-0458-4>.
- [73] Y. Wang, T. Seppänen-Laakso, H. Rischer, M.G. Wiebe, Euglena gracilis growth and cell composition under different temperature, light and trophic conditions, PLoS ONE 13 (2018) e0195329. <https://doi.org/10.1371/journal.pone.0195329>.
- [74] F. Ivušić, B. Šantek, Optimization of complex medium composition for heterotrophic cultivation of Euglena gracilis and paramylon production, Bioprocess Biosyst. Eng. 38 (2015) 1103–1112. <https://doi.org/10.1007/s00449-015-1353-3>.
- [75] R.E. Hurlbert, S.C. Rittenberg, Glucose Metabolism of Euglena gracilis var. bacillaris; Growth and Enzymatic Studies*, J. Protozool. 9 (1962) 170–182. <https://doi.org/10.1111/j.1550-7408.1962.tb02602.x>.
- [76] J. Chen, L. Liu, P.-E. Lim, D. Wei, Effects of sugarcane bagasse hydrolysate (SCBH) on cell growth and fatty acid accumulation of heterotrophic Chlorella protothecoides, Bioprocess Biosyst. Eng. 42 (2019) 1129–1142. <https://doi.org/10.1007/s00449-019-02110-z>.
- [77] X.-M. Shi, X.-W. Zhang, F. Chen, Heterotrophic production of biomass and lutein by Chlorella protothecoides on various nitrogen sources, Enzyme Microb. Technol. 27 (2000) 312–318. [https://doi.org/10.1016/S0141-0229\(00\)00208-8](https://doi.org/10.1016/S0141-0229(00)00208-8).
- [78] A. Huang, L. Sun, S. Wu, C. Liu, P. Zhao, X. Xie, G. Wang, Utilization of glucose and acetate by Chlorella and the effect of multiple factors on cell composition, J. Appl. Phycol. 29 (2017) 23–33. <https://doi.org/10.1007/s10811-016-0920-6>.

- [79] M. Sakarika, M. Kornaros, Effect of pH on growth and lipid accumulation kinetics of the microalga *Chlorella vulgaris* grown heterotrophically under sulfur limitation, *Bioresour. Technol.* 219 (2016) 694–701. <https://doi.org/10.1016/j.biortech.2016.08.033>.
- [80] X. Shi, Z. Wu, F. Chen, Kinetic modeling of lutein production by heterotrophic *Chlorella* at various pH and temperatures, *Mol. Nutr. Food Res.* 50 (2006) 763–768. <https://doi.org/10.1002/mnfr.200600037>.
- [81] W. Kong, H. Song, Y. Cao, H. Yang, S. Hua, C. Xia, The characteristics of biomass production, lipid accumulation and chlorophyll biosynthesis of *Chlorella vulgaris* under mixotrophic cultivation, *Afr. J. Biotechnol.* 10 (2011) 11620–11630.
- [82] J.L. Yáñez, J.A. Mateos, P. Santolaria, Tris buffer improves fluorescence yield of ram spermatozoa when evaluating membrane integrity, *Microsc. Res. Tech.* 75 (2012) 520–523. <https://doi.org/10.1002/jemt.21086>.
- [83] K. Hosotani, T. Ohkochi, H. Inui, A. Yokota, Y. Nakano, S. Kitaoka, Photoassimilation of Fatty Acids, Fatty Alcohols and Sugars by *Euglena gracilis* Z, *Microbiology* 134 (1988) 61–66. <https://doi.org/10.1099/00221287-134-1-61>.
- [84] J. Lacroux, J. Seira, E. Trably, N. Bernet, J.-P. Steyer, R. Van Lis, Mixotrophic Growth of *Chlorella sorokiniana* on Acetate and Butyrate: Interplay Between Substrate, C:N Ratio and pH, *Front. Microbiol.* 12 (2021) 703614. <https://doi.org/10.3389/fmicb.2021.703614>.
- [85] M. Casal, O. Queirós, G. Talaia, D. Ribas, S. Paiva, Carboxylic Acids Plasma Membrane Transporters in *Saccharomyces cerevisiae*, in: J. Ramos, H. Sychrová, M. Kschischo (Eds.), *Yeast Membr. Transp.*, Springer International Publishing, Cham, 2016: pp. 229–251. https://doi.org/10.1007/978-3-319-25304-6_9.
- [86] J. Lacroux, E. Trably, N. Bernet, J.-P. Steyer, R. van Lis, Mixotrophic growth of microalgae on volatile fatty acids is determined by their undissociated form, *Algal Res.* 47 (2020) 101870. <https://doi.org/10.1016/j.algal.2020.101870>.
- [87] J. Trček, N.P. Mira, L.R. Jarboe, Adaptation and tolerance of bacteria against acetic acid, *Appl. Microbiol. Biotechnol.* 99 (2015) 6215–6229. <https://doi.org/10.1007/s00253-015-6762-3>.
- [88] G. Curien, D. Lyska, E. Guglielmino, P. Westhoff, J. Janetzko, M. Tardif, C. Hallopeau, S. Brugière, D. Dal Bo, J. Decelle, B. Gallet, D. Falconet, M. Carone, C. Remacle, M. Ferro, A.P.M. Weber, G. Finazzi, Mixotrophic growth of the extremophile *Galdieria sulphuraria* reveals the flexibility of its carbon assimilation metabolism, *New Phytol.* 231 (2021) 326–338. <https://doi.org/10.1111/nph.17359>.
- [89] C. Chen, Q. Shi, A. Tong, L. Sun, J. Fan, Screening of microalgae strains for efficient biotransformation of small molecular organic acids from dark fermentation biohydrogen production wastewater, *Bioresour. Technol.* 390 (2023) 129872. <https://doi.org/10.1016/j.biortech.2023.129872>.
- [90] N. Kishimoto, K. Inagaki, T. Sugio, T. Tano, Growth inhibition of *Acidiphilium* species by organic acids contained in yeast extract, *J. Ferment. Bioeng.* 70 (1990) 7–10. [https://doi.org/10.1016/0922-338X\(90\)90021-N](https://doi.org/10.1016/0922-338X(90)90021-N).
- [91] C. Baker-Austin, M. Dopson, Life in acid: pH homeostasis in acidophiles, *Trends Microbiol.* 15 (2007) 165–171. <https://doi.org/10.1016/j.tim.2007.02.005>.
- [92] L.C. Rai, J.P. Gaur, eds., *Algal Adaptation to Environmental Stresses*, Springer Berlin Heidelberg, Berlin, Heidelberg, 2001. <https://doi.org/10.1007/978-3-642-59491-5>.
- [93] J. Zhu, M. Wakisaka, Effect of two lignocellulose related sugar alcohols on the growth and metabolites biosynthesis of *Euglena gracilis*, *Bioresour. Technol.* 303 (2020) 122950. <https://doi.org/10.1016/j.biortech.2020.122950>.
- [94] X. Huang, Y. Wen, Y. Chen, Y. Liu, C. Zhao, Structural characterization of *Euglena gracilis* polysaccharide and its in vitro hypoglycemic effects by alleviating insulin resistance, *Int. J. Biol. Macromol.* 236 (2023) 123984. <https://doi.org/10.1016/j.ijbiomac.2023.123984>.
- [95] E.C. O’Neill, M. Trick, L. Hill, M. Rejzek, R.G. Dusi, C.J. Hamilton, P.V. Zimba, B. Henrissat, R.A. Field, The transcriptome of *Euglena gracilis* reveals unexpected metabolic capabilities for

- carbohydrate and natural product biochemistry, *Mol. Biosyst.* 11 (2015) 2808–2820. <https://doi.org/10.1039/C5MB00319A>.
- [96] K.J. Fox, K.L. Prather, Carbon catabolite repression relaxation in *Escherichia coli*: global and sugar-specific methods for glucose and secondary sugar co-utilization, *Curr. Opin. Chem. Eng.* 30 (2020) 9–16. <https://doi.org/10.1016/j.coche.2020.05.005>.
- [97] B. Görke, J. Stülke, Carbon catabolite repression in bacteria: many ways to make the most out of nutrients, *Nat. Rev. Microbiol.* 6 (2008) 613–624. <https://doi.org/10.1038/nrmicro1932>.
- [98] M.A. Mechoud, N. Pujol-Carrion, S. Montella-Manuel, M.A. De La Torre-Ruiz, Interactions of GMP with Human Glrx3 and with *Saccharomyces cerevisiae* Grx3 and Grx4 Converge in the Regulation of the Gcn2 Pathway, *Appl. Environ. Microbiol.* 86 (2020) e00221-20. <https://doi.org/10.1128/AEM.00221-20>.
- [99] A. Nair, S.J. Sarma, The impact of carbon and nitrogen catabolite repression in microorganisms, *Microbiol. Res.* 251 (2021) 126831. <https://doi.org/10.1016/j.micres.2021.126831>.
- [100] W.A. Wilson, S.A. Hawley, D.G. Hardie, Glucose repression/derepression in budding yeast: SNF1 protein kinase is activated by phosphorylation under derepressing conditions, and this correlates with a high AMP:ATP ratio, *Curr. Biol.* 6 (1996) 1426–1434. [https://doi.org/10.1016/S0960-9822\(96\)00747-6](https://doi.org/10.1016/S0960-9822(96)00747-6).
- [101] J. Chen, X. Liu, D. Wei, G. Chen, High yields of fatty acid and neutral lipid production from cassava bagasse hydrolysate (CBH) by heterotrophic *Chlorella protothecoides*, *Bioresour. Technol.* 191 (2015) 281–290. <https://doi.org/10.1016/j.biortech.2015.04.116>.
- [102] J. Mu, S. Li, D. Chen, H. Xu, F. Han, B. Feng, Y. Li, Enhanced biomass and oil production from sugarcane bagasse hydrolysate (SBH) by heterotrophic oleaginous microalga *Chlorella protothecoides*, *Bioresour. Technol.* 185 (2015) 99–105. <https://doi.org/10.1016/j.biortech.2015.02.082>.
- [103] J.E. Gonzalez, C.P. Long, M.R. Antoniewicz, Comprehensive analysis of glucose and xylose metabolism in *Escherichia coli* under aerobic and anaerobic conditions by ¹³C metabolic flux analysis, *Metab. Eng.* 39 (2017) 9–18. <https://doi.org/10.1016/j.ymben.2016.11.003>.
- [104] V. Novy, R. Wang, J.O. Westman, C.J. Franzén, B. Nidetzky, *Saccharomyces cerevisiae* strain comparison in glucose–xylose fermentations on defined substrates and in high-gravity SSCF: convergence in strain performance despite differences in genetic and evolutionary engineering history, *Biotechnol. Biofuels* 10 (2017) 205. <https://doi.org/10.1186/s13068-017-0887-9>.
- [105] H.G. Lawford, J.D. Rousseau, Effect of oxygen on ethanol production by a recombinant ethanologenic *E. coli*, *Appl. Biochem. Biotechnol.* 45–46 (1994) 349–366. <https://doi.org/10.1007/BF02941811>.
- [106] A. Andreeva, E. Budenkova, O. Babich, S. Sukhikh, E. Ulrikh, S. Ivanova, A. Prosekov, V. Dolganyuk, Production, Purification, and Study of the Amino Acid Composition of Microalgae Proteins, *Molecules* 26 (2021) 2767. <https://doi.org/10.3390/molecules26092767>.
- [107] E.E. Andeden, S. Ozturk, B. Aslim, Effect of alkaline pH and nitrogen starvation on the triacylglycerol (TAG) content, growth, biochemical composition, and fatty acid profile of *Auxenochlorella protothecoides* KP7, *J. Appl. Phycol.* 33 (2021) 211–225. <https://doi.org/10.1007/s10811-020-02311-0>.
- [108] M.S. Roth, D.J. Westcott, M. Iwai, K.K. Niyogi, Hexokinase is necessary for glucose-mediated photosynthesis repression and lipid accumulation in a green alga, *Commun. Biol.* 2 (2019) 347. <https://doi.org/10.1038/s42003-019-0577-1>.
- [109] M. Martinez-Garcia, M.J.E.C. Van Der Maarel, Floridoside production by the red microalga *Galdieria sulphuraria* under different conditions of growth and osmotic stress, *AMB Express* 6 (2016) 71. <https://doi.org/10.1186/s13568-016-0244-6>.
- [110] E. Suzuki, R. Suzuki, Variation of Storage Polysaccharides in Phototrophic Microorganisms, *J. Appl. Glycosci.* 60 (2013) 21–27. https://doi.org/10.5458/jag.jag.JAG-2012_016.

- [111] C. Plancke, H. Vigeolas, R. Höhner, S. Roberty, B. Emonds-Alt, V. Larosa, R. Willamme, F. Duby, D. Onga Dhali, P. Thonart, S. Hiligsmann, F. Franck, G. Eppe, P. Cardol, M. Hippler, C. Remacle, Lack of isocitrate lyase in *C. hlamydomonas* leads to changes in carbon metabolism and in the response to oxidative stress under mixotrophic growth, *Plant J.* 77 (2014) 404–417. <https://doi.org/10.1111/tpj.12392>.
- [112] K. Mozaffari, M. Seger, B. Dungan, D.T. Hanson, P.J. Lammers, F.O. Holguin, Alterations in photosynthesis and energy reserves in *Galdieria sulphuraria* during corn stover hydrolysate supplementation, *Bioresour. Technol. Rep.* 7 (2019) 100269. <https://doi.org/10.1016/j.biteb.2019.100269>.
- [113] I. Lang, L. Hodac, T. Friedl, I. Feussner, Fatty acid profiles and their distribution patterns in microalgae: a comprehensive analysis of more than 2000 strains from the SAG culture collection, *BMC Plant Biol.* 11 (2011) 124. <https://doi.org/10.1186/1471-2229-11-124>.
- [114] M.A. Hazrat, M.G. Rasul, M. Mofijur, M.M.K. Khan, F. Djavanroodi, A.K. Azad, M.M.K. Bhuiya, A.S. Silitonga, A Mini Review on the Cold Flow Properties of Biodiesel and its Blends, *Front. Energy Res.* 8 (2020) 598651. <https://doi.org/10.3389/fenrg.2020.598651>.
- [115] T. Heredia-Arroyo, W. Wei, B. Hu, Oil Accumulation via Heterotrophic/Mixotrophic *Chlorella protothecoides*, *Appl. Biochem. Biotechnol.* 162 (2010) 1978–1995. <https://doi.org/10.1007/s12010-010-8974-4>.
- [116] W. Kong, S. Yang, H. Wang, H. Huo, B. Guo, N. Liu, A. Zhang, S. Niu, Regulation of biomass, pigments, and lipid production by *Chlorella vulgaris* 31 through controlling trophic modes and carbon sources, *J. Appl. Phycol.* 32 (2020) 1569–1579. <https://doi.org/10.1007/s10811-020-02089-1>.
- [117] E. Korozi, V. Tsagou, I. Kefalogianni, G. Markou, D. Antonopoulos, L. Chakalis, Y. Kotzamanis, I. Chatzipavlidis, Continuous Culture of *Auxenochlorella protothecoides* on Biodiesel Derived Glycerol under Mixotrophic and Heterotrophic Conditions: Growth Parameters and Biochemical Composition, *Microorganisms* 10 (2022) 541. <https://doi.org/10.3390/microorganisms10030541>.
- [118] A. Wei, X. Zhang, D. Wei, G. Chen, Q. Wu, S.-T. Yang, Effects of cassava starch hydrolysate on cell growth and lipid accumulation of the heterotrophic microalgae *Chlorella protothecoides*, *J. Ind. Microbiol. Biotechnol.* 36 (2009) 1383–1389. <https://doi.org/10.1007/s10295-009-0624-x>.

CRedit authorship contribution statement

Pablo Perez Saura: Writing – original draft, Writing – review & editing, Conceptualization, Methodology. Claire Remacle: Conceptualization, Methodology, Writing – review & editing, Supervision, Funding acquisition. Pierre Cardol: Writing – review & editing. Stéphanie Gérin: Writing – review & editing. All authors read and approved the final manuscript.

Conflict of Interest

The authors declare that the research was conducted in the absence of any commercial or financial relationships that could be construed as a potential conflict of interest.

Acknowledgments

This work was supported by Fonds de la Recherche Scientifique (FNRS) (CDR J.0175.20 to CR and n°40020920 to PC; PDR n°33663953 to PC) ; Fonds Wetenschappelijk Onderzoek – Vlaanderen (FWO) and FNRS under the Excellence of Science (EOS) Project No. 30829584; Action de Recherche Concertée from the University of Liege (DARKMET ARC grant 17/21-08), and ADV_BIO grant (SPF Économie, P.M.E., Classes moyennes et Énergie, Direction générale de l'Énergie). We thank M. Radoux for expert technical assistance. We would also like to extend our thanks to Clarisse Varisano for her valuable contribution to the experiments during her internship.

Data availability

Data will be made available on request.

Declaration of Generative AI and AI-assisted technologies in the writing process

During the preparation of this work the author(s) used ChatGPT (OpenAI) for its assistance in linguistic and grammatical improvement of the manuscript. After using this tool, the authors reviewed and edited the content as needed and take full responsibility for the content of the publication.

Tables description

Table 1. Comparison of the molecules and elements concentrations between the 2xGS Allen and TMP media. Values are expressed in molar units (M) and do not include pH adjustment. NF: the compound is not found in the medium.

Table 2. Growth parameters of *G. sulphuraria*, *E. gracilis*, or *A. protothecoides* in the presence of different substrates. Data are presented as means of three independent biological replicates \pm SD. NG: no growth was observed for that strain and condition. The clover symbol (♣) indicates values for *G. sulphuraria* grown on glucose from a previous study conducted in our laboratory [20].

Table 3. Fatty acids distribution in exponential and stationary phases when growth was observed in the presence of glucose, xylose, acetate or a mix of the three carbon sources for *G. sulphuraria*, *E. gracilis*, or *A. protothecoides*. SFA, saturated fatty acids; MUFA, mono-unsaturated fatty acids; PUFA, poly-unsaturated fatty acids. Data are expressed as a percentage of the FA species on the total FAs detected. Values represent the means \pm SD (n=3). ND: the FA species was not detected. The clover symbol (♣) indicates values for *G. sulphuraria* grown on glucose from a previous study conducted in our laboratory [20].

Figure legend

Figure 1. Schematic representation of the uptake and metabolism of glucose, xylose, acetate, and ammonium (NH_4^+) in microalgae, based on [14,20,36–42,60]. Black arrows indicate specific enzymatic reactions leading to the subsequent products (enzyme names and co-substrates are generally not specified). Black arrows crossing trapezoids represent transporters. Small gray arrows connect single compounds that can be transferred from one pathway to another. Circular dashed arrows represent metabolic cycles (with intermediate products and enzymatic reactions not shown), and straight dashed arrows indicate entry points into specific metabolic pathways written in bold and italics, which are not necessarily detailed. Orange and blue arrows mark specific reactions of glycolysis and gluconeogenesis, respectively. The dashed arrows connecting xylose to xylulose omitting the xylitol intermediate represent the putative presence of a xylose isomerase, as already characterized in bacteria [61]. Compound abbreviations are specified as follows: α -KG, α -ketoglutarate; ACP, acyl carrier protein; AMT1, ammonium transporter 1; CoA, coenzyme A; DHA-P, dihydroxyacetone phosphate; FA, fatty acid; G3P, glyceraldehyde 3-P; Gln, glutamine; Glu, glutamate; HUP1-2, hexose uptake protein; MCT, monocarboxylate transporters; MFS, major facilitator superfamily; PEP, phosphoenolpyruvate; PPP, pentose phosphate pathway; TAG, triacylglycerol; TCA, tricarboxylic acid. The locations where metabolic reactions occur have intentionally not been specified, as they may differ depending on the species studied.

Figure 2. Growth curves, and evolution of carbon sources concentration and pH in the culture media of *G. sulphuraria* (light blue diamonds), *E. gracilis* (orange triangles), and *A. protothecoides* (dark green squares) cells grown in heterotrophy in the presence of glucose (A-B), xylose (C-D), or acetate (E-F). Graphs (A,C,E) show dry weight evolution (gDW L^{-1} - solid

lines, secondary vertical axis) and carbon source concentration in the media (mM of carbon atoms - dashed lines, primary vertical axis) over time (days). Graphs (B,D,F) show the pH evolution in cultures (pH units - dashed lines, primary horizontal axis) over time (days). Each value on the graphs is presented as the mean of three independent biological replicates. Error bars represent standard deviation of the mean (\pm SD). The clover symbol (♣) indicates values for *G. sulphuraria* grown on glucose from a previous study conducted in our laboratory [20].

Figure 3. Growth curves, and evolution of carbon sources concentration and pH in the culture media of *G. sulphuraria* (light blue diamonds), *E. gracilis* (orange triangles), and *A. protothecoides* (dark green squares) cells grown in heterotrophy in the presence of a mix of glucose, xylose and acetate (A-D). Graphs (A) shows dry weight evolution (gDW L⁻¹ - solid lines, secondary vertical axis) and carbon source concentrations in the media (mM of total carbon atoms - dashed lines, primary vertical axis) over time (days). Graphs (B) show the pH evolution in cultures (pH units - dashed lines, primary vertical axis) over time (days). Graphs (C) and (D) show the glucose (dashed line, light gray circles) xylose (dashed line, dark gray circles), and acetate (dashed line, black circles) consumption (mM of carbon atoms – primary vertical axis) over time (days) in cultures of *E. gracilis* or *A. protothecoides*, respectively. In graph (D), the inset shows the carbon source evolution from day 0 to day 1. Each value on the graphs is presented as the mean of three independent biological replicates. Error bars represent standard deviation of the mean (\pm SD).

Figure 4. Total fatty acids, storage polysaccharides (glycogen, paramylon or starch), and protein content of *G. sulphuraria* (light blue bars), *E. gracilis* (orange bars), and *A. protothecoides* (dark green bars) cultures grown in heterotrophy in the presence of glucose, xylose, acetate, or a mix of the three carbon sources, during exponential or stationary phases.

Bar charts (A) and (B) show the protein and storage polysaccharide content in biomass (expressed in g gDW⁻¹), respectively. Bar chart (C) shows the fatty acids content in biomass (expressed in mg gDW⁻¹). Data represent the mean of three independent biological replicates. Error bars represent the standard deviation of the mean (\pm SD). The clover symbol (♣) indicates values for *G. sulphuraria* grown on glucose from a previous study conducted in our laboratory [20].

Supplemental files

Figure S1. Ammonium (NH_4^+ , dotted lines – primary vertical axis) and phosphate (PO_4^{3-} , dashed lines – secondary vertical axis) concentrations upon time in cultures media of *G. sulphuraria* (light blue diamonds), *E. gracilis* (orange triangles), and *A. protothecoides* (dark green squares) cells grown in heterotrophy in the presence of glucose (A), xylose (B), acetate (C), or a mix of the three carbon sources (D). Data are expressed in mM. Each value on the graphs is presented as the mean of three independent biological replicates. Error bars represent standard deviation of the mean (\pm SD). The clover symbol (\clubsuit) indicates values for *G. sulphuraria* grown on glucose from a previous study conducted in our laboratory [20].

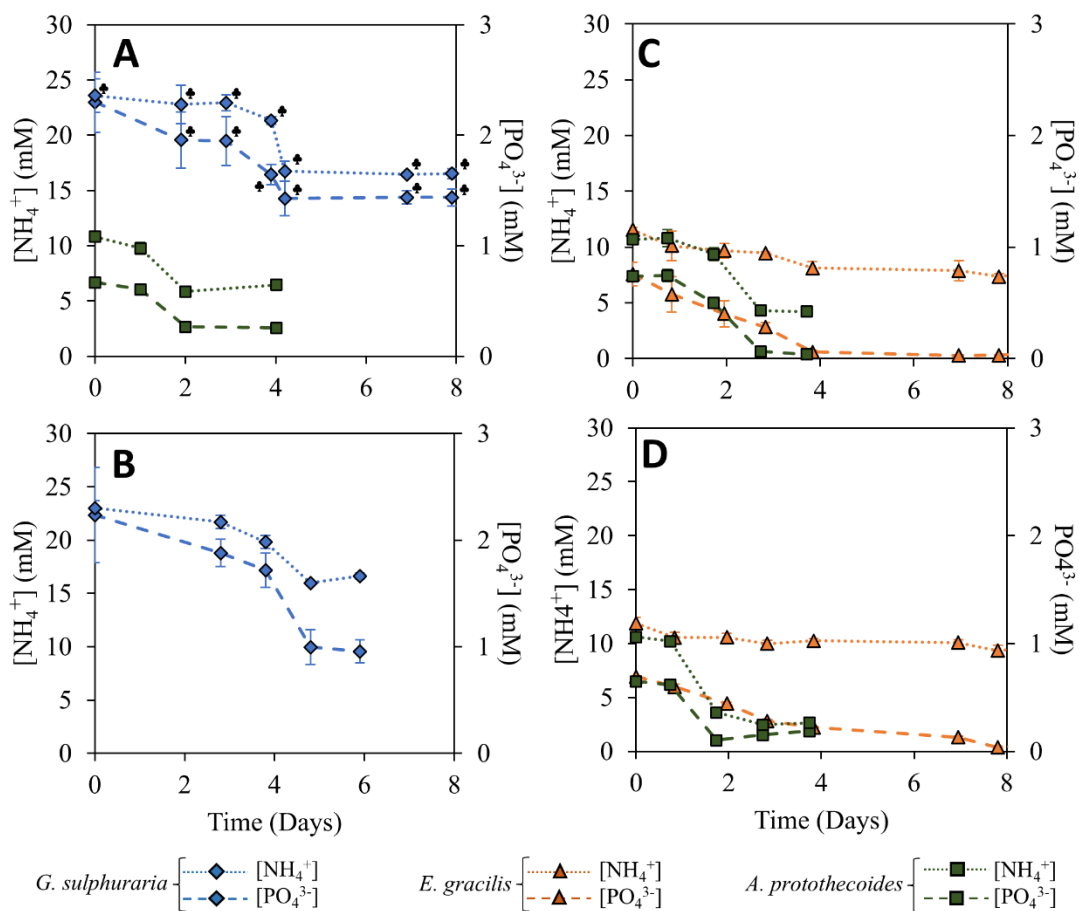


Table S1. Pigment content and distribution in exponential and stationary phase when growth was observed in the presence of glucose, xylose, acetate or a mix of the three carbon sources for *G. sulphuraria*, *E. gracilis*, or *A. protothecoides*. Data are expressed in mg gDW⁻¹. Values represent the means ± SD (n=3). NF: The pigment does not exist in the microalgal species. ND: The pigment can be found but was not detected during this study. The clover symbol (♣) indicates values for *G. sulphuraria* grown on glucose from a previous study conducted in our laboratory [20].

Growth phase	Pigment content (mg gDW ⁻¹)	Glucose		Xylose		Acetate		Mix	
		<i>G. sulphuraria</i>	<i>A. protothecoides</i>	<i>G. sulphuraria</i>	<i>A. protothecoides</i>	<i>E. gracilis</i>	<i>A. protothecoides</i>	<i>E. gracilis</i>	
Exponential	Neoxanthin	NF	0.014 ± 0.007	NF	0.012 ± 0.011	ND	0.005 ± 0.001	ND	
	Violaxanthin	NF	0.019 ± 0.003	NF	0.006 ± 0.005	ND	0.003 ± 0.000	ND	
	Antheraxanthin	NF	0.015 ± 0.006	NF	0.002 ± 0.002	ND	0.001 ± 0.000	ND	
	Lutein	ND	0.187 ± 0.005	ND	0.099 ± 0.007	ND	0.072 ± 0.006	ND	
	Zeaxanthin	0.164 ± 0.002 ♣	0.0863 ± 0.005	0.126 ± 0.005	0.038 ± 0.008	ND	0.030 ± 0.004	ND	
	Chlorophyll <i>b</i>	NF	0.0145 ± 0.003	NF	0.102 ± 0.024	ND	0.029 ± 0.005	ND	
	Chlorophyll <i>a</i>	0.354 ± 0.001 ♣	0.075 ± 0.009	0.200 ± 0.002	0.311 ± 0.036	ND	0.089 ± 0.013	ND	
	β-carotene	0.064 ± 0.005 ♣	0.012 ± 0.011	0.042 ± 0.002	ND	ND	ND	ND	
	Phycocyanin	1.048 ± 0.275 ♣	NF	0.765 ± 0.158	NF	NF	NF	NF	
Stationary	Neoxanthin	NF	ND	NF	0.005 ± 0.001	ND	0.011 ± 0.001	ND	
	Violaxanthin	NF	ND	NF	0.001 ± 0.000	ND	0.002 ± 0.000	ND	
	Antheraxanthin	NF	ND	NF	0.001 ± 0.000	ND	0.001 ± 0.000	ND	
	Lutein	ND	0.037 ± 0.001	ND	0.055 ± 0.002	ND	0.070 ± 0.002	ND	
	Zeaxanthin	0.270 ± 0.007 ♣	0.012 ± 0.001	0.239 ± 0.039	0.021 ± 0.001	ND	0.021 ± 0.003	ND	
	Chlorophyll <i>b</i>	NF	0.016 ± 0.001	NF	0.034 ± 0.001	ND	0.063 ± 0.008	ND	
	Chlorophyll <i>a</i>	0.528 ± 0.159 ♣	0.030 ± 0.001	0.487 ± 0.189	0.158 ± 0.009	ND	0.215 ± 0.020	ND	
	β-carotene	0.115 ± 0.003 ♣	0.051 ± 0.007	0.091 ± 0.028	ND	ND	ND	ND	
	Phycocyanin	1.818 ± 0.037 ♣	NF	2.275 ± 0.262	NF	NF	NF	NF	

NF: The pigment does not exist in the microalgal species. ND: The pigment can be found but was not detected during this study.

Table S2. Cell density, carbon source concentration, and pH, after 7 days of cultures of *E. gracilis* strain Z grown in KH or TMP medium in the presence of glucose or acetate (50 mMC) at different starting pH values. Initial inoculum density was set at 125000 cells/mL. Data are expressed as the mean of two independent biological replicates \pm SD.

Medium	KH				TMP			
Starting pH	3.5		7.5		3.5		7.5	
Carbon source	Acetate	Glucose	Acetate	Glucose	Acetate	Glucose	Acetate	Glucose
Cell density (10^3 cells mL ⁻¹)	135 \pm 21	1530 \pm 71	375 \pm 35	145 \pm 7	155 \pm 21	100 \pm 14	525 \pm 64	98 \pm 3
Carbon source concentration (mMC)	53.2 \pm 0.6	8.0 \pm 3.2	3.1 \pm 0.1	57.1 \pm 1.6	7.2 \pm 0.6	59 \pm 2.6	10.4 \pm 0.3	54.7 \pm 3.0
Is growth observed ?	NO	YES	YES	NO	NO	NO	YES	NO